NOTICE

AVIS

The quality of this microform is heavily dependent upon the quality of the original thesis submitted for microfilming. Every effort has been made to ensure the highest quality of reproduction possible.

La qualité de cette microforme dépend grandement de la qualité de la thèse soumise au microfilmage. Nous avons tout fait pour assurer une qualité supérieure de reproduction.

If pages are missing, contact the university which granted the degree.

S'il manque des pages, veuillez communiquer avec l'université qui a conféré le grade.

Some pages may have indistinct print especially if the original pages were typed with a poor typewriter ribbon or if the university sent us an inferior photocopy.

La qualité d'impression de certaines pages peut laisser à désirer, surtout si les pages originales ont été dactylographiées à l'aide d'un ruban usé ou si l'université nous a fait parvenir une photocopie de qualité inférieure.

Canada

University of Alberta

The Preparation and Acoustic Properties of Silica Aerogels

by

Ying Xie   ©

A thesis submitted to the Faculty of Graduate Studies and Research in partial fulfillment

of the requirements for the degree of Master of Science

in

Solid State Physics

Department of Physics

Edmonton, Alberta

Fall, 1995

THE AUTHOR HAS GRANTED AN
IRREVOCABLE NON-EXCLUSIVE
LICENCE ALLOWING THE NATIONAL
LIBRARY OF CANADA TO
REPRODUCE, LOAN, DISTRIBUTE OR
SELL COPIES OF HIS/HER THESIS BY
ANY MEANS AND IN ANY FORM OR
FORMAT, MAKING THIS THESIS
AVAILABLE TO INTERESTED
PERSONS.

L'AUTEUR A ACCORDE UNE LICENCE
IRREVOCABLE ET NON EXCLUSIVE
PERMETTANT A LA BIBLIOTHEQUE
NATIONALE DU CANADA DE
REPRODUIRE, PRETER, DISTRIBUER
OU VENDRE DES COPIES DE SA
THESE DE QUELQUE MANIERE ET
SOUS QUELQUE FORME QUE CE SOIT
POUR METTRE DES EXEMPLAIRES DE
CETTE THESE A LA DISPOSITION DES
PERSONNE INTERESSEES.

THE AUTHOR RETAINS OWNERSHIP
OF THE COPYRIGHT IN HIS/HER
THESIS. NEITHER THE THESIS NOR
SUBSTANTIAL EXTRACTS FROM IT
MAY BE PRINTED OR OTHERWISE
REPRODUCED WITHOUT HIS/HER
PERMISSION.

L'AUTEUR CONSERVE LA PROPRIETE
DU DROIT D'AUTEUR QUI PROTEGE
SA THESE. NI LA THESE NI DES
EXTRAITS SUBSTANTIELS DE CELLE-
CI NE DOIVENT ETRE IMPRIMES OU
AUTREMENT REPRODUITS SANS SON
AUTORISATION.

Canada

University of Alberta
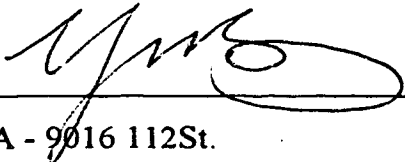
Library Release Form

Name of Author: Ying Xie

Title of Thesis: The Preparation and Acoustic Properties of Silica Aerogels

Degree: Master of Science

Year this Degree Granted: 1995

Permission is hereby granted to the University of Alberta Library to reproduce single copies of this thesis and to lend or sell such copies for private, scholarly, or scientific research purposes only.

The author reserves all other publication and other rights in association with the copyright in the thesis, and except as hereinbefore provided, neither the thesis nor any substantial portion thereof may be printed or otherwise reproduced in any material form whatever without the auther's prior written permission.

3A - 9016 112St.
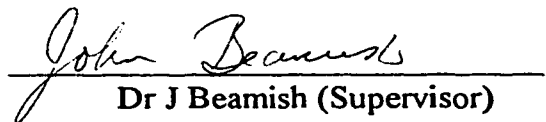
Edmonton, Alberta, T6G 2C5, Canada

Date: Aug. 30th, 1995
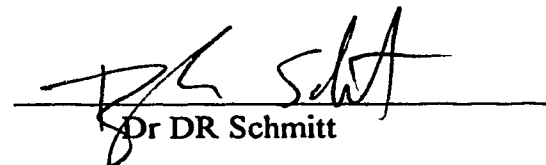
THE UNIVERSITY OF ALBERTA

FACULTY OF GRADUATE STUDIES AND RESEARCH

The undersigned certify that they have read, and recommend to the Faculty of Graduate Studies and Research for acceptance, a thesis entitled *The Preparation and Acoustic Properties of Silica Aerogels* submitted by Ying Xie in partial fulfilment for the degree of Master of Science in Solid State Physics.

Dr J Beamish (Supervisor)

Dr JP Franck

Dr DR Schmitt

Dr A Mar

Date: June 29, 1995

DEDICATION

This dissertation is dedicated to my parents, Zong-lin Xie and Wan-bi Zhong

ACKNOWLEDGEMENTS

TABLE OF CONTENTS

Chapter

LIST OF FIGURES

LIST OF TABLES

ABSTRACT

Silica aerogels are highly porous materials. The samples of silica aerogels with porosities from 87% to 98% have been produced by using one-step method in laboratory scale. The ultrasonic measurements on variations of attenuations and sound velocities with respect to temperature have been made on silica aerogel samples at all temperature from room temperature to 14K and at the frequencies from 3 MHZ to 18.5 MHZ. A huge attenuation peak was observed around 60K - 80K, and correspondingly a big change in sound velocity is also detected at the temperature where the attenuation peak occurs.

Chapter 1   INTRODUCTION

Aerogels are extremely porous materials. They contain pores or voids and allow fluids to penetrate through one side and emerge on the other. In aerogels' family there are aerogels of either silica, alumina, xirconia, stannic or tungsten oxide or mixtures of these oxides. Due to their high porosity and their large surface area, aerogels are used as active catalysts or catalytic substrates, adsorbents, fillers, reinforcement agents, pigments and gellifying agents.

The production of aerogels starts with a sol-gel conversion, which is the development of a polymer network from a chemical solution while the whole cross-linked structure is still submerged in a liquid. A so-called supercritical drying process follows, which removes the liquid without the delicate structure shrinking or collapsing.

Silica aerogel, one of the most common aerogels, is characterized as "an open, cross-linked silica structure with a high fraction of voids with extremely fine pore sizes"[1.1]. It is very light, transparent and resilient. Two important structural parameters of porous materials are the porosity, which for silica aerogel is extremely high, up to 99%, and the specific surface area, which is also very high, typically 600 to 800 m^2/g[1.2].

Like other aerogels, silica aerogels can be used as catalysts, adsorbents, fillers, etc. Moreover, thanks to its transparency, silica aerogel can be used as insulation in window

systems to significantly reduce thermal losses. It is also used to improve the energy balance in passive solar systems.

Besides these commercial applications, silica aerogel is of interest to physicists for two main reasons: its fractal structure and its effect on phase transitions in liquids confined within its pores. Over a wide range of densities, silica aerogels form self-similar volume fractals. The fractal dimension of a neutrally prepared or acid-catalyzed aerogel is about 2.40 ± 0.03[1.3]. Moreover, because of its extremely low density, it is much more convenient to observe the fractal behavior in aerogels than in other disordered solids. As for phase transitions of liquids in aerogels, those of liquid helium are typical and have been studied in many experiments. For liquid helium, the effects of confinement and randomness on its phase transitions have been seen in its isotropic phase separation[1.4], its suppressed superfluidity, and its depressed freezing point[1.5]. The critical behavior is quite different from that of bulk helium, e.g., different critical exponents for the superfluid density[1.6] and cusplike heat-capacity singularities[1.7].

The study of the propagation of sound waves in aerogels is also an interesting subject. Aerogels themselves are fascinating materials with unique acoustic properties. They have extremely low sound velocities, especially aerogels with high porosity, due to their exceptionally small elastic moduli. Acoustic measurements are also often used in the study of fluids in pores, for example, second sound in superfluid helium.

Only a few acoustic measurements have been made on aerogels. Calemczuk *et al.*[1.8] measured room temperature longitudinal and transverse sound velocities on low density samples at ultrasonic frequencies (f~10 MHz) using a pulse echo method. Some ultrasonic measurements were also made by Gross *et al.*[1.9] on samples with densities in the range 0.005 - 0.5 g/cm³. Ultrasonic transducers were used for transmitting and receiving signals. For low density samples, frequencies of 33-200 KHz were used, while for samples with densities above 0.05 g/cm³, the frequencies were 1-5 MHz. de Goer *et al.* have made measurements of elastic modulus and acoustic attenuation on low density samples (ρ = 0.27 - 0.87 g/cm³) at low frequency (3 kHz) and low temperature (100 mK - 70 K) by using a resonant bar method[1.10]. Up until now there have not been any measurements of the temperature dependence of the sound velocity and attenuation at MHz frequencies and low frequency (kHz) measurements have only been made at low temperatures (below 70 K).

The work in this thesis consists of two parts: making silica aerogels and ultrasonic measurements on aerogels. By using a "one-step" process, silica aerogels were made with porosities from 0.87 to 0.98. Ultrasonic measurements were made on several of these as well as on one aerogel produced elsewhere. The measurements include longitudinal and transverse sound velocities at room temperature as well as the temperature dependence of the velocities and attenuations from room temperature to 14 K. Measurements were made at frequencies from 3 MHz to 18.5 MHz and for both longitudinal and transverse modes. This is the first time that acoustic measurements have been made on aerogels over such a large temperature and frequency range.

This thesis contains six chapters:

Chapter 1. Introduction

Chapter 2. Properties of Aerogels

Chapter 3. Sound Propagation in Aerogels

Chapter 4. Experimental Methods

       - production of aerogels

       - cryogenics

       - ultrasonics and sample preparation

       - ultrasonic measurements

Chapter 5. Results

       - aerogels produced

       - ultrasonic velocity and attenuation

Chapter 6. Conclusions.

Chapter 2   PROPERTIES OF AEROGELS

§ 2.1   Production of Silica Aerogel

Silica aerogels were first produced in 1931 by Kistler, whose use of a hypercritical drying process to replace the liquid in a gel by a gas (air) without the pores collapsing and shrinking was the breakthrough for the development of a new generation of high-performance porous solids.

Generally, the process of making a silica aerogel consists of two major parts: gelation and drying. The gelation process is a chemical reaction which results in a gel (or alcogel) submerged in a solvent, sometimes with impurities. Of course, the impurities are the first things to get rid of. In order to carry out the hypercritical drying process, the solvent should be something other than water, preferably something with a lower critical point like methanol. A catalyst may be used to speed up the reaction or improve the quality of the alcogel. After gelation the alcogel is placed into an autoclave and the second part of the process begins, hypercritical drying. In this part the solvent is removed above its critical temperature and pressure so that no liquid-vapor meniscus is present to shrink or crack the gel structure.

Kistler's work[2.1] started with chemical reaction:

$$Na_2SiO_3 + 2\ HCl\ (aq) \rightarrow SiO_2, nH_2O + 2\ NaCl, \qquad [1]$$
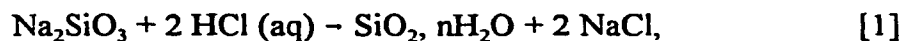
which required a process of firstly washing the "impurities" Na^+ and Cl^- out of the aquagel and then changing the solvent from water to methanol or ethanol. It was very time consuming and tedious. At that time, it took a week to make a single silica aerogel sample. However, his hypercritical drying process was extremely successful. He could easily prepare aerogels with densities as low as 0.1 g/cm^3 and even some with a density of only 0.02 g/cm^3.

In 1968, Teichner introduced a new method of making silica aerogels by dissolving tetramethoxysilane (TMOS, $Si(OCH_3)_4$) in methanol and hydrolysing it by adding a controlled amount of water:[2.2]

$$Si(OCH_3)_4 + 4\ H_2O \rightarrow SiO_2, 2H_2O + 4\ CH_3OH. \qquad [2]$$

This speeded up the process of making aerogel since it was not necessary to wash the gel and replace the solvent, so that production took only a couple of days.

After the sol to gel procedure described above, the key procedure in making an aerogel is hypercritical drying, a process which is used to replace the alcohol in the gel structure by air without causing collapse and shrinkage. In a conventional drying process, both liquid and vapor phases of methanol exist so liquid vapor interfaces form in the pores of the gel structure. The surface tension of the liquid meniscus applies a force on the wall of the

pores equivalent to a pressure of the order of 20000 kg/cm^2 for a capillary of 2 nm diameter. As a result, the porous structure collapses by closing of capillaries or shrinking of small particles.[2.2]

The hypercritical drying process consists of letting the gel dry in an autoclave above the critical point of methanol (Tc = 239.5 °C, P = 80.9 psi) so that there will no longer be a liquid-vapor meniscus in the capillaries. This process, shown in Fig. 1, starts with heating. When the temperature increases from room temperature, the pressure increases too since the methanol is confined to a small volume. Heating continues until both the temperature and the pressure of the system are above the critical point, e.g., T=270 °C, P=149.6 bar (2200 psi), point B on figure 1. Then the methanol is slowly released from the gel while the temperature is held at 270 °C until the pressure reaches one atmosphere, point C. The residual methanol is then evacuated by a roughing pump. Finally, the system is cooled to room temperature while pumping (point D). This process avoid the collapse and shrinkage simply because there is no chance to form a liquid-vapor interface in the capillaries. This hypercritical drying process results in a highly porous silica aerogel with density as low as 0.01 g/cm^3. Its surface area is typically 1000 m^2/g, with strands of silica particles about 2 nm in diameter [2.2].

This one-step procedure is easily generalized to make not only silica aerogel but also other inorganic oxide aerogels, either pure or a mixture of oxides.

Aerogel is also manufactured on a large scale. Two groups were involved in the
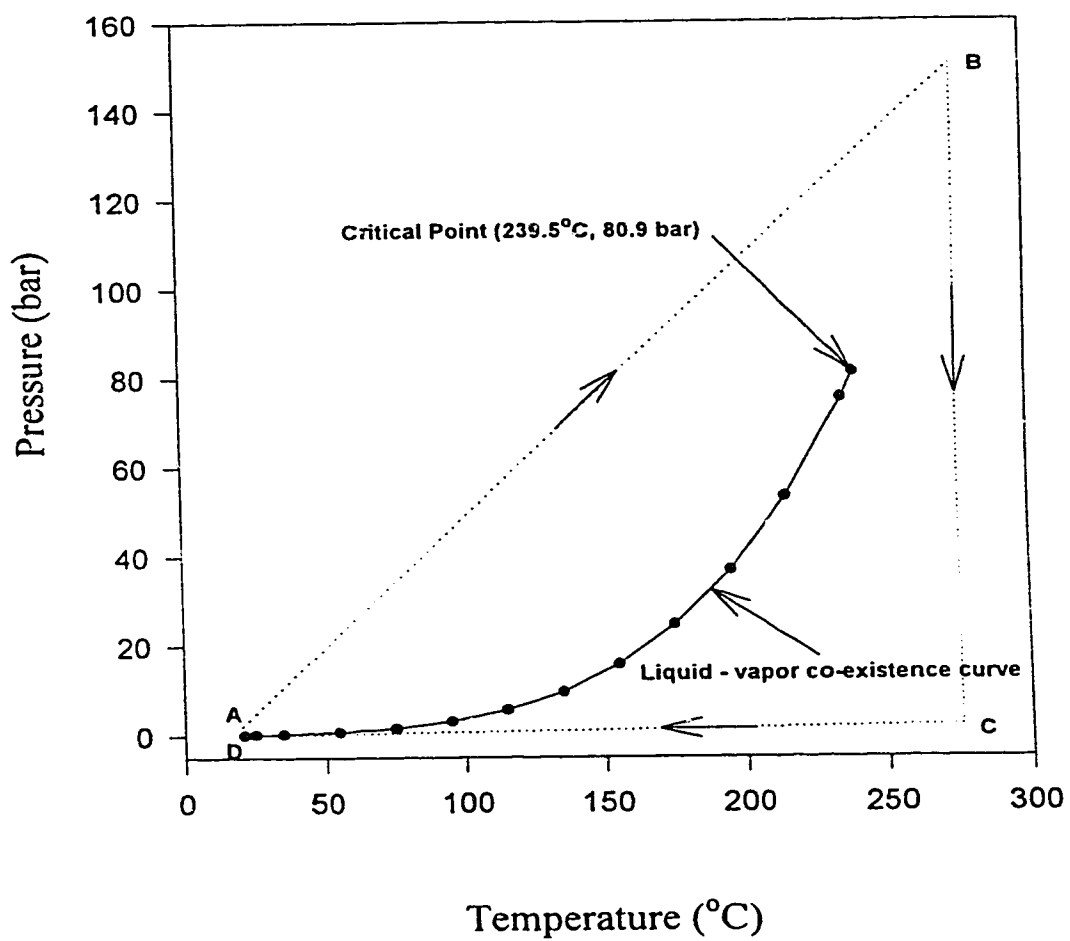
Fig. 1 The liquid - vapor co-existence curve of methanol

production of clear crack-free transparent silica aerogel tiles of low density using the above method. One, at DESY in Hamburg, produced about 1700 l of aerogel with a very low index of refraction (1.024) in 1981[2.3]. Another, at the University of Lund in Sweden, provided about 1000 l of aerogel with refractive index of 1.050 in 1976[2.4]. Both of them used similar procedures, first gelation, secondly covering the alcogel with mixture of methanol and water and aging it for 10 days after it gelled, thirdly hypercritically drying the gels for 35 hours and finally baking the aerogels for 2 hours at 400 °C to get rid of the residual methoxyl groups on their internal surfaces.

§ 2.2   Characterization

Silica aerogel is a porous material, with characteristics which are quite different from those of the bulk silica. Moreover, its properties vary widely depending on the exact nature of the pore network, or the way in which the solid elements are arranged. It can be characterized using the conventional methods used for porous materials. To describe a porous material, two types of parameters are commonly used: macroscopic and microscopic. Both are completely determined by the pore structure. Macroscopic parameters represent average behavior of a sample containing many pores, the three most important of which are porosity, permeability and specific surface area. Microscopic parameters are those which describe the actual pore structure, such as grain size and pore size.

2.2.1. Porosity

The porosity of a material is simply the pore volume, V_p, divided by the total volume, V_t. There are two ways to find the porosity. The first is simply a density measurement. The geometrical volume and the mass are measured to get the porous material's density ρ_p, which is then compared to the density of the bulk constituent material, ρ_s. The porosity ϕ is:

$$\phi = 1 - \rho_p/\rho_s. \qquad [3]$$

The second standard method is the three weight method. This method is more accurate since it is much simpler and more accurate to measure weight than volume. The three measurements performed here are the weight of the sample, W_s, the weight of the sample completely saturated with a fluid, W_f, and the apparent weight of the saturated sample while submerged in the fluid, W_b. The three measurements give the porosity as

$$\phi = (W_f - W_s) / (W_s - W_b). \qquad [4]$$

The density method must be used to find the porosity of aerogels because it is really hard to find a fluid which will not damage aerogels.

2.2.2. Specific surface area

The specific surface area of a porous material is defined as "the interstitial surface area of the void and pores either per unit mass or per unit bulk volume"[2.5].

The most common method of measuring the surface area is gas adsorption. The volume of gas (usually N_2 at its normal boiling point) which is adsorbed is measured and the resulting adsorption isotherm is analyzed by using the famous BET method[2.6]. The BET method is used by almost every group studying aerogels to find surface area[2.7].

2.2.3. Grain size and pore size

The "grains" here refer to the particles which form the materials, while the "pores" are the voids. In the case of silica aerogel, the grain actually is the silica sphere mentioned above. Owing to the great irregularity of the pore geometry, pore size is an simplification of reality; a distribution of pore sizes makes much more sense here.

Direct imaging is the most obvious way to study pore structure. The scanning electron microscope (SEM) and the transmission electron microscope (TEM) are often used to see what the structures look like and to measure the grain size as well. The pore size, or more appropriately the distribution of pore sizes, can be determined from the BET isotherms for adsorption and desorption of N_2. Scattering measurements, such as small-angle neutron-scattering (SANS), small angle X-ray scattering (SXRS) and light scattering have also been used to study the structure of porous materials, especially the smallest particles and voids.

2.2.4. Fractal structure

A fractal structure is one which is "neither a line nor a surface but rather an object with fractional (non-integer) dimension"[2.8]. It is self-similar, which means that it looks the same at any magnification. Aerogels often form self-similar volume fractals, mathematically cluster fractals, in which case, the mass M within a scale L has a power law dependence ($M \sim L^D$). D here is called the fractal dimension and can be a non-integer number. For a homogeneous solid, D = 3. For a volume fractal, D is usually smaller than 3. Fractal structure in silica aerogels appears over a range of length scales from about 5 Å to 200 or 300 Å, depending on their porosity and the pH value of the starting solution. The fractal structure has been observed by small-angle neutron-scattering (SANS) in which the fractal dimension can be calculated from the total scattered intensities as a function of the scattering vector.

§ 2.3   Structure

Silica aerogel, according to Poelz and Riethmuller[2.3], "consists of small spheres of amorphous silica bound together to branched strings forming a three-dimensional network the pores of which are filled with air", as shown in Fig. 2.
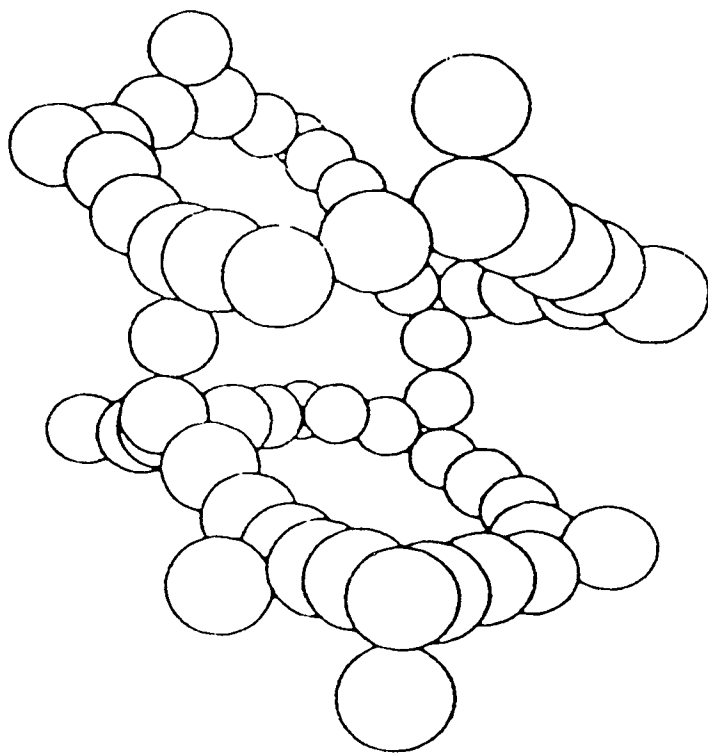
Fig. 2   Schematic drawing showing the structure of silica aerogel[2,3]

The spheres in this picture are about 4 nm in diameter. There is a pore diameter distribution extending from a few nm to a few hundred nm[2.9]. The micropores (d < 20 nm) occupy a volume of 0.6 - 0.8 cm³/g, and combined with the mesopores (20 nm < d < 60 nm) occupy 1.2 - 1.8 cm³/g, which is about 15% of the total pore volume in high porosity aerogels (ϕ = 95%) and almost 50% for lower porosity aerogels (ϕ = 88%). The macropores (d > 60 nm, up to about 1 µm) are the major part (50% to 85%) of the total pore volume[1.11].

Silica aerogels form fractal structure. Self-similar volume fractals are seen in silica aerogel over a range of length scales L from the diameter of a mean particle (a homogeneous microcluster), a, to a correlation length ξ, the average root square distance between those clusters. The size a and their spatial arrangement depend on the pH value during gelation. For neutrally prepared aerogels the fractal dimension is D = 2.40 ± 0.01, while for non-neutrally prepared gels fractal dimensions of D = 1.9 and D = 2.4 are found for base catalyzed and acid catalyzed gels respectively[1.3].

§ 2.4   Properties

Aerogels are highly inhomogeneous materials. Their density can be as low as 0.2% of that of amorphous silica (2.19 g/cm³) and therefore their physical properties are strikingly different from those of solid silica. They also depend strongly upon the preparation procedures, e.g. the pH value of the solution, aging time and baking time.

2.4.1. Thermal properties

Thermal properties of insulators are usually related to their acoustic properties since phonons are involved. The thermal conductivity λ and specific heat C_p of silica aerogels are very different from those of solid silica. They are, for example, 0.0131 W/m-K and 0.74 kJ/kg-K respectively[2.9] at room temperature for a sample with density $\rho=0.109$ g/cm^3.

The thermal conductivities and specific heats have been measured by Calemczuk *et al.*[1.8] at low temperatures, 0.1-10 K, for silica aerogels of various densities. The thermal conductivity is shown in Fig. 3 along with that for solid amorphous silica. The curves in this figure show that the thermal conductivity increases with both temperature and density; the lowest-density aerogel has the smallest conductivity. Furthermore, the shapes of the curves are similar for the aerogels but different from that of bulk SiO$_2$. The specific heat data are presented in Fig. 4 as C_p/T^3 versus T. Below 2 K, all the curves are similar in shape. The most dense gel (c) has a heat capacity ~~it shows~~ $C_p \sim T^{1.1}$ which is the same in bulk glasses, but the values for aerogels are about 50 times bigger than those of bulk SiO$_2$. All the data are well below the Debye specific heats (calculated from the density and sound speeds) which are indicated by arrows. This is not unexpected, since sound velocities are measured at long wavelengths but the phonons responsible for the specific heat have wavelengths smaller than the pore sizes, except at extremely low temperatures.

2.4.2. Acoustic properties
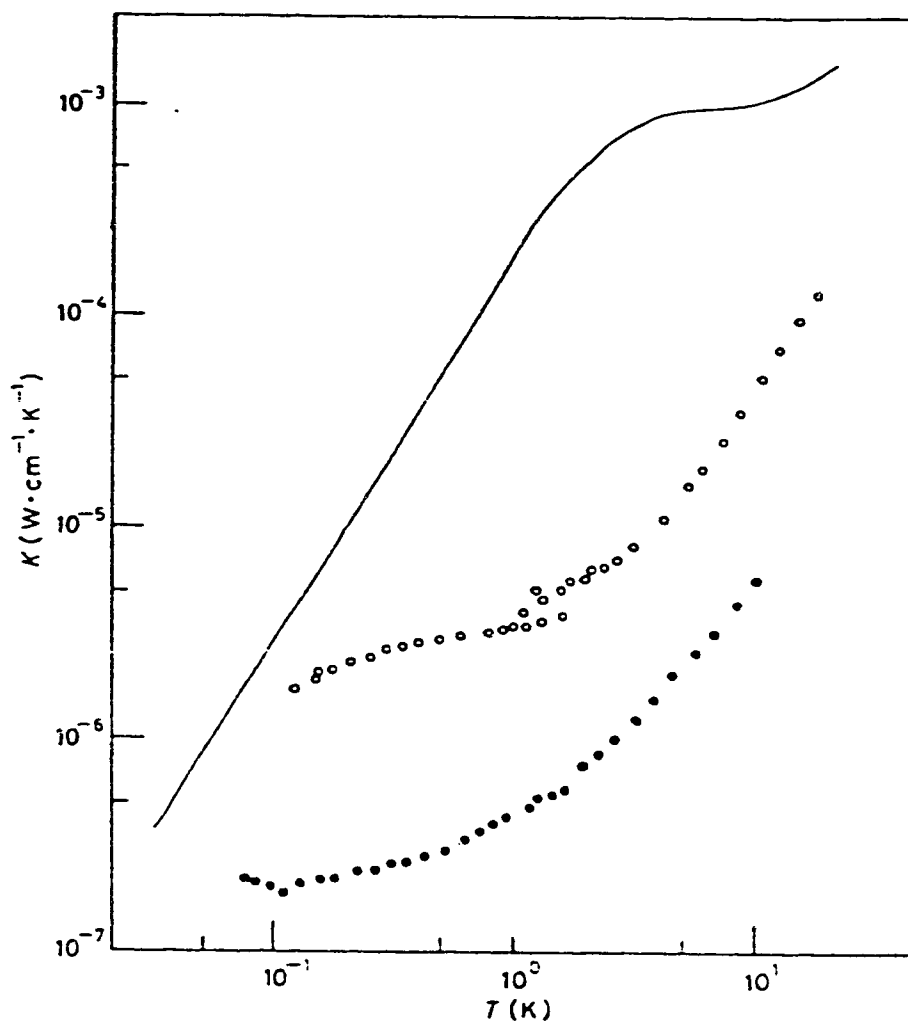
Fig. 3 Thermal conductivity of silica aerogels. ○: 0.87 g/cm^3,●: 0.27 g/cm^3, solid line:

Bulk α-SiO$_2$[1.8]
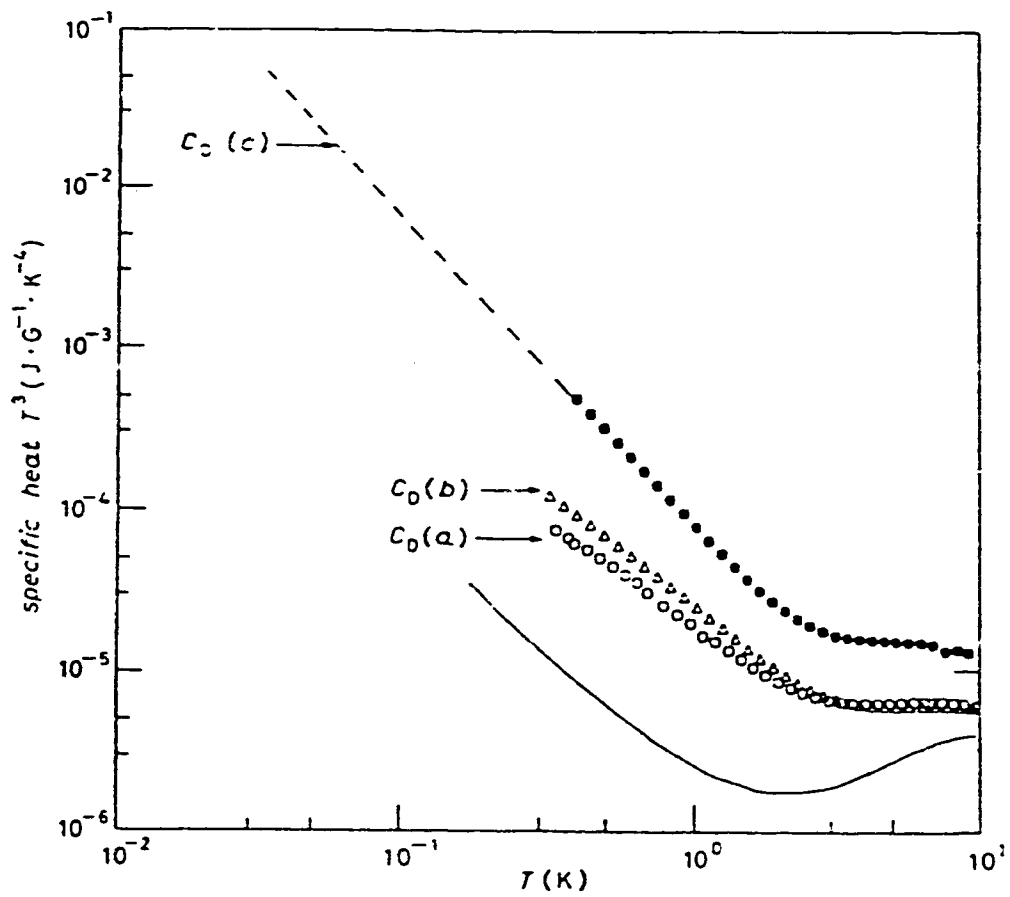
Fig. 4 Specific heat of silica aerogels. o: 0.87 g/cm^3(c), △: 0.72 g/cm^3(b), ●: 0.27 g/cm^3(a), solid line: Bulk α-SiO$_2$[1.8]

The acoustic properties of aerogels are fascinating. Scund velocities can be as low as 20 m/s thanks to the exceptionally small elastic moduli. The Young's modulus measured in static experiments varies as a power of the density with a rather large exponent $(\rho^{3.8})$[1.9]. Since the density ρ is very low, so is the Young's modulus (10^6-10^7 N/m^2). One conclusion that can be drawn from the sound velocity measurements is that, for $\phi < 98\%$, the sound is carried by the silica skeleton, and not by air in the pores of the gel.[1.1]

Chapter 3   SOUND PROPAGATION IN AEROGELS

Sound waves are energy in the form of mechanical vibrations which propagate in a medium. Acoustics is the study of sound waves and ultrasonics is the part dealing with frequencies above 20,000 Hz. Ultrasonic techniques have many applications not only in physics research but also in everyday life. This chapter is an overall introduction to sound propagation in solids, glasses, porous materials and finally aerogels.

§ 3.1   Sound Propagation in Solids

In a homogeneous, isotropic, elastic solid, three sound waves can exist: one longitudinal wave and two transverse waves. The longitudinal wave is one in which the direction of particle motion is the same as its propagation direction, whereas transverse waves are those in which the direction of vibration is normal to their propagation direction. The sound velocity of a longitudinal wave is

$$v_l = [(K_s + 4/3\mu_s)/\rho_s]^{1/2}; \qquad [5]$$

and that of a transverse wave is

$$v_t = (\mu_s/\rho_s)^{1/2}, \qquad [6]$$

where K_s is the bulk modulus of the material, μ_s is the shear modulus and the ρ_s is the density. Ideally, in an elastic medium without damping or other losses, the sound velocities are independent of frequency and the amplitude of the sound wave is constant for a plane wave, no matter how far away it is from the source.

In real solids, however, there is dispersion in the sound velocity and attenuation due to various inelastic processes, e.g. the absorption of energy by defects, and reflection, refraction, diffraction and scattering[3.11]. Absorption is a process in which sound is transformed into other sorts of energy. It can be due to lattice defects (impurities and dislocations), thermoplastic effects, electron-phonon and phonon-phonon interactions, magnetoelastic interactions in ferromagnetic or ferroelectric materials and the thermoplastic relaxation and grain boundary losses in amorphous or polymer materials. Energy losses from reflection, refraction, diffraction and scattering are determined by the geometry of the system and the physical properties of the medium or media. Reflection and refraction occur at boundaries between areas with different acoustic impedances. Diffraction occurs where there are obstacles in the way of the propagating sound wave. Scattering depends on deviations of the elastic properties and density from point to point in the solid.

In many cases, a sound wave interacts with the internal structure of a solid through some sort of relaxation process. In a relaxation process, the attenuation (the energy loss of the sound wave to the medium) exhibits a peak when $\omega\tau = 1$, i.e. when the relaxation time τ is roughly equal to the sound period. The change in sound velocity is related to the

attenuation. It is smallest at low frequencies and largest at high frequencies, with the crossover occuring at $\omega\tau = 1$, the position of the attenuation peak. Generally, the attenuation due to a thermally activated relaxation process with an activation energy V can be calculated by using the following formula[3.2]:

$$l^{-1} = \frac{D^2}{4\rho v^3 kT} \int_0^\infty P(V) \frac{\omega^2 \tau(V)}{1 + \omega^2 \tau^2(V)} dV \qquad [7]$$

where l^{-1} is the attenuation, D is the deformation potential, ρ is the density, v is the sound velocity, ω is the angular frequency of the sound wave, τ is the relaxation time, and P(V) is the distribution function. The corresponding variation of the sound velocity is

$$\frac{\Delta v}{v} = \frac{D^2}{8\rho v^2 kT} \int_0^\infty P(V) \frac{dV}{1 + \omega^2 \tau^2(V)}. \qquad [8]$$

§3.2 Sound Propagation in Glasses

Since aerogels are amorphous, the acoustic properties of glasses are of great interest here. Glasses have quite different acoustic properties from crystalline solids but all glasses behave similarly, especially at low temperatures.

The temperature dependence of the attenuation of sound is shown in Fig. 5[3.2] for longitudinal waves in vitreous (amorphous) silica (a and b) and in crystalline quartz (c). The attenuation curves for vitreous silica are very different from that for the crystal. There is a huge, broad absorption peak around 50 K in each of the glass curves, but none in the curve of the crystal. This peak shifts to slightly higher temperature when the frequency of the sound wave increases. The absorption per wave length is nearly the same for longitudinal and transverse waves. Similar absorption is seen in other glasses as shown in Fig. 6[3.3]. Moreover, at low temperature, around 5 K, there is significant shoulder on each of the glass curves followed by a rapid decrease in attenuation at lower temperature. In the crystal there is almost no absorption in the low temperature range (below 20 K).

The variation of sound velocity with temperature is presented in Fig. 7[3.2]. The changes in sound velocity of longitudinal waves in glasses are quite large and are both positive and negative. At the lowest temperatures shown, the sound velocity in all glasses decreases with increasing temperature. For tetrahedrally bonded glasses such as SiO_2, BeF_2, GeO_2 and $Zn(PO_3)$, the sound velocity reaches a minimum at a temperature a little higher than the attenuation peak then increases linearly at higher temperatures. Further measurements show that, at very low temperature, the attenuation becomes intensity-dependent[3.2], saturating with increasing intensity. However, this is typically only observed at lower temperature (<1 K) and higher frequencies (>100 MHz) than those used in the acoustic measurements in this thesis.

The striking difference between the attenuation in glasses and crystals indicates that
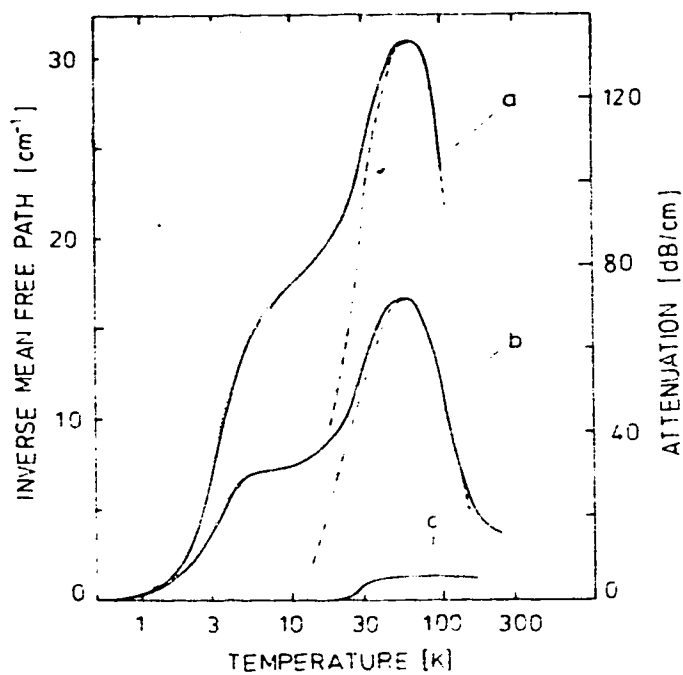
Fig. 5 Temperature dependence of the attenuation of longitudinal sound waves in vitreous

silica and a quartz crystal. Glass: (a) 930 MHz, (b) 507 MHz, Crystal: (c) 1000 MHz,

dashed lines: theoretical fits[3.2].
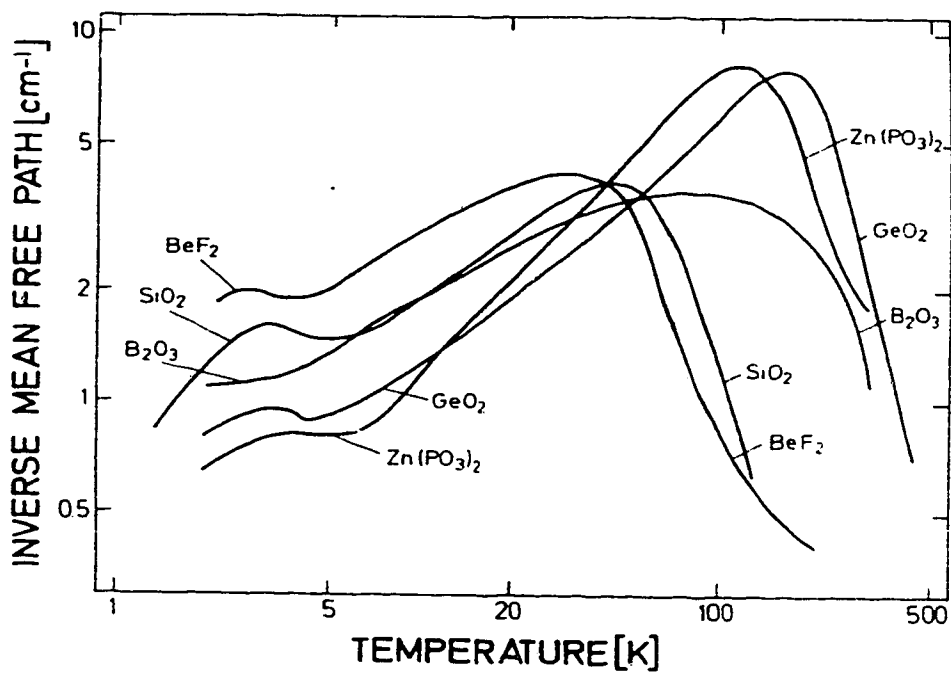
Fig. 6 Acoustic attenuation (or inverse mean free path) of several glasses below room

temperature (Longitudinal, 20MHz)[3.3].
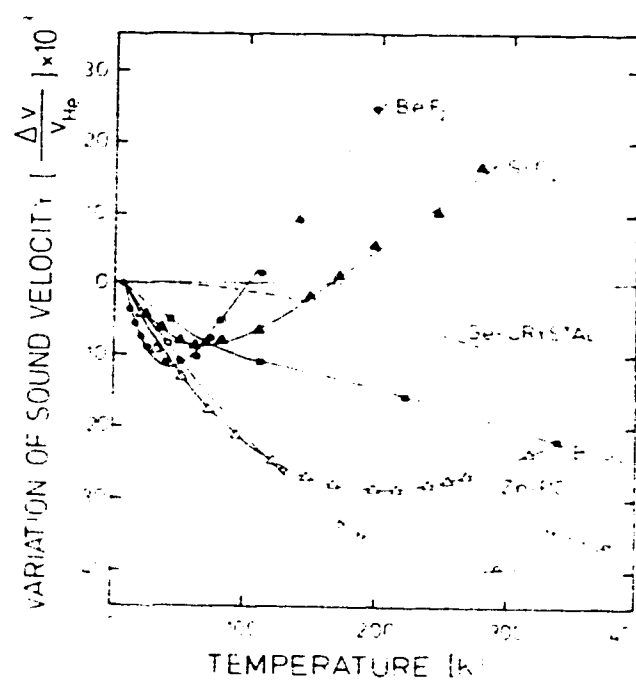
Fig. 7 Fractional temperature variation of the sound velocity in glasses and a crystal[3.2]

there must be a different attenuation mechanism in glasses. One, proposed by Anderson and Bömmel (1955), is a relaxation process with a thermally activated relaxation time τ given by the Arrhenius relationship as

$$\tau = \tau_0 \, exp \, (V/kT) \qquad\qquad [9]$$

where τ_0 is a constant with a value of order 10^{-13} second and V is the activation energy which must be roughly 570 K[3.2] to explain the frequency dependence of the peak position (the peak appears at the temperature where $\omega\tau = 1$). The attenuation can be calculated using equation [7] along with equation [9]. The results of the calculations[3.2] are shown in Fig. 5 by the dashed lines, from which one can see that a relaxation process can explain the results very well.

This thermally activated relaxation process is also thought to be the reason the sound velocity in glasses decreases with increasing temperature. The variation of sound velocity can also be calculated by using equation [8] and [9]. However, this process seems less convincing in explaining the linear velocity increase at higher temperatures in tetrahedrally bonded glasses.

From a microscopic point of view, this thermally activated relaxation process is based on a model of a particle moving in a double-well potential. Vibrating with frequency of τ_0^{-1} in one minimum of the potential, this particle can overcome the barrier between the two wells

via a thermally activated process. The distribution of activation energies for this process is equivalent to the distribution of the barrier heights. In vitreous silica, X-ray scattering[3.3] indicates a structure like that shown in Fig. 8(b). The oxygen atom can occupy two equilibrium positions (A or B on Fig. 8(b)) which correspond to the two potential minima. The distribution of double-well barriers is due to the disordered structure of the vitreous silica, unlike the crystalline form crystobalite, shown for comparison in Fig. 8(a), which has long-range order so that each oxygen atom sits in exactly the same potential well.

At temperatures below 10 K, the absorption (attenuation) of the sound wave, shown in Fig. 5, has a shoulder or peak around 5 K, which is also quite different from the attenuation in crystals. At still lower temperatures the attenuation decreases rapidly as T^3. A new mechanism common to all amorphous materials is thought to be responsible for this behavior. This mechanism is referred to as "two-level systems" (TLS) and is also responsible for low temperature anomalies in the sound velocity.

Two-level systems are low-energy excitations which are assumed to have a nearly constant density of states in glasses. Microscopically, a two-level system also corresponds to a double-well potential. However, since it is important at very low temperature, it must have a comparatively low potential barrier. This results in tunneling between potential wells and therefore splittings in the energies of states.

These two-level systems have a large influence on sound propagation in glasses at low
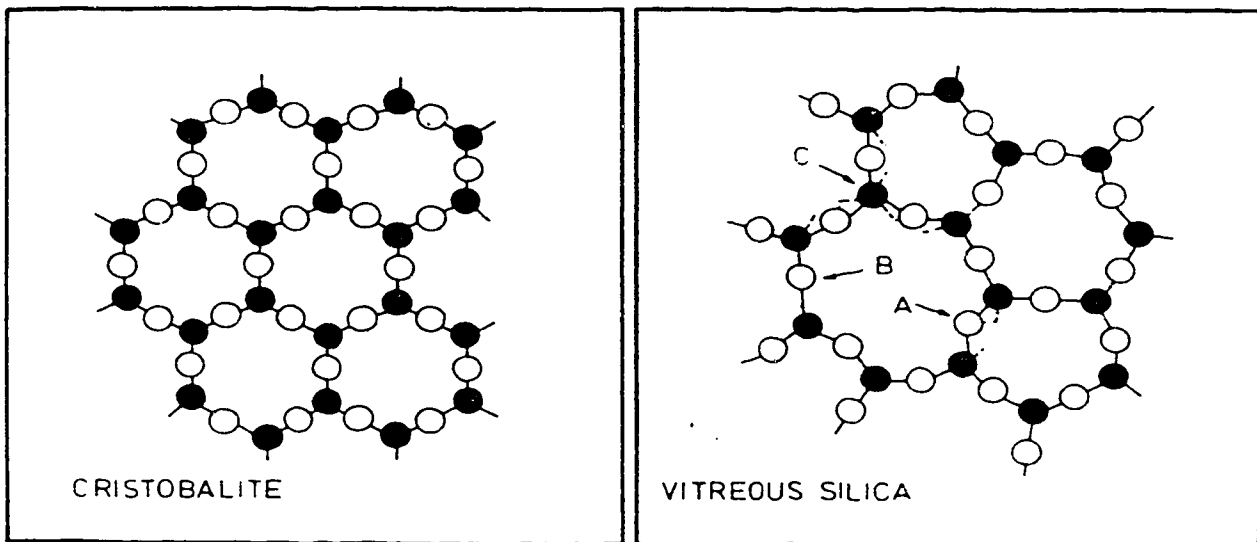
Fig. 8 Schematic two-dimensional representation of the structure of cristobalite, a crystalline modification of SiO_2, and of vitreous silica. ●:Si atoms, ○:O atoms[3.3]

temperatures. There are two sorts of absorption related to two-level systems: resonant and relaxation. The resonant interaction of a sound wave with a two-level system is a one-phonon process in which a two-level system absorbs a phonon and re-emits it again after a recombination time τ_1. This absorption is amplitude-dependent. With increasing acoustic intensity, the upper level becomes more populated so, effectively, there are fewer two-level systems available to absorb phonons and hence the absorption decreases. There also is a relaxation absorption. At higher temperatures, a sound wave disturbs the thermal equilibrium population of the two-level systems and then the systems relax back to a new equilibrium by absorbing and emitting thermal phonons. This is a power-independent process since all the thermally activated two-level systems are involved in this process, not just those resonant with the sound wave. It has a totally different temperature dependence from that of resonant direct absorption[3,4].

By treating a two-level system as equivalent to a spin system, the attenuations due to both resonant and relaxation processes can be calculated[3,2]. As an example, in the low-temperature limit, where $\omega\tau_1 \gg 1$, the attenuation due to relaxation is:

$$\alpha_{rel} = \frac{\pi^3 k^3 T^3 \tau(4,0.5)}{2\rho h^4 v^3} n_a D^2 \left(\frac{M_l^2}{v_l^5} + \frac{2M_t^2}{v_t^5}\right) \tag{10}$$

where $\tau(4, 0.5) = 97.38$ is the Riemann zeta function, n_a is the number of the states for acoustically active systems (assumed to be a constant), M and D are deformation potentials

(coupling constants) and v_t and v_l are the sound speeds. From this one can see that at low temperatures the relaxation attenuation is proportional to T^3, in agreement with experimental results such as those shown in Fig. 5.

Figure 9 shows typical changes in sound velocity at very low temperatures. There is a maximum at about 2 K, below which the sound velocity decreases logarithmically with temperature. The resonant and relaxation absorptions together provide an explanation of this behavior. Which of these competing interactions is dominant depends on the temperature and sound frequency. Above the maximum, the relaxation process dominates and below it, the resonant process dominates[3.2]. The variation of sound velocity also can be calculated[3.2] and the result is shown by dashed lines in Fig. 9, which agree well with the experimental results. In addition, specific heat measurements show a contribution from two-level systems at low temperatures, so that the model provides a successful description of the low temperature thermal and acoustic properties of glasses.

§ 3.3   Sound Propagation in Porous Materials

Porous materials such as aerogels consist of a network of solid containing interconnected voids. If the pore diameter, d, is much smaller than the sound wavelength λ, then the pores do not scatter the sound wave and the medium can be treated as homogeneous. However, the porous structure still has an influence on sound propagation. For a material
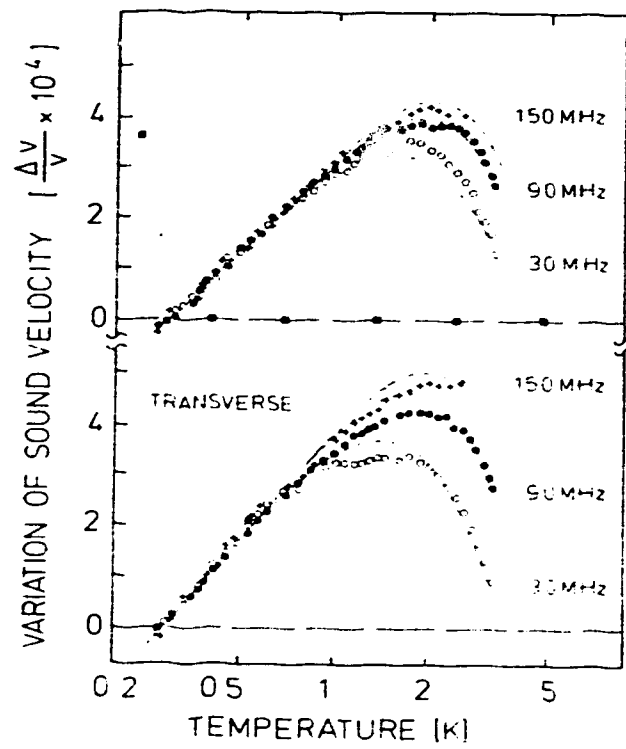
Fig. 9   Relative variation of longitudinal and transverse sound velocity in borosilicate glass

BK7[3.2]

with porosity ϕ, the sound velocities v_l and v_t decrease with increasing ϕ, because of the strong dependence of elastic moduli on ϕ. The porous medium's density is

$$\rho_p = (1 - \phi)\rho_s,$$ [11]

and its elastic moduli are

$$\mu_p < \mu_s$$ [12]

$$K_p < K_s.$$ [13]

However, K_p and μ_p, which depend on pore structure, decrease with ϕ faster than ρ_p does. Cracks, for example, affect the moduli much more than they affect the density[3,5].

§ 3.4   Sound Propagation in Aerogels

The acoustic properties of aerogels' depend strongly on its porosity (or density). The Young's modulus of silica aerogels is proportional to a large power of the density, ρ^α, where $\alpha \sim 3.6$ for densities $\rho < 0.1$ g/cm^3 and $\alpha \sim 2.6$ for $\rho > 0.1$ g/cm^3 [1,9]. The corresponding longitudinal sound velocity varies as $v_l \sim \rho^\beta$, where $\beta \sim 1.3$ and 0.8 in the different density ranges. Thus the sound velocity can be very small when the density is low. For an aerogel with density 0.005 g/cm^3 ($\phi \sim 99.8\%$), the velocity of a longitudinal sound wave v_l is as small

as 20 m/s, compared to 5968 m/s for solid silica ($\phi = 0$). The density dependence of the sound velocity can be seen in Table 1 as an example.

Density ρ (g/cm^3)	v_l (m/s)	v_t (m/s)
0.87	1850	1180
0.72	1500	960
0.27	425	260

Table 1. The density dependence of the sound velocity[1.8]

It has also been shown that both heat treatment of aerogels and air contained in their pores can have a significant influence on sound velocities. A sintered aerogel is much stiffer (and so has higher sound velocities) than untreated one with the same density[1.9]. According to the work of Mulder and van Lierop[3.6], the density of an aerogel increases when it is heated above 800°C. Air in the pores of an aerogel increases the sound velocity by about 5% in a aerogel with density ρ=0.1 g/cm^3 but can be neglected for higher density aerogels [1.9]. This indicates that sound propagates mainly through the solid network. The contribution of air can be substantial for low density samples. For example, in the 0.005 g/cm^3 sample, the sound velocity with air in the pores was 152 m/s, compared to 20 m/s when the sample was evacuated. For an aerogel containing gas at pressure p_{gas} and density ρ_{gas}, the longitudinal sound velocity can be expressed as[3.7]

$$v_l^2 = \frac{(K_a + 4\mu_d/3) + (1/\phi)(1 - K_d/K_s)^2 p_{gas}}{\rho_a + \phi\rho_{gas}}$$

[14]

showing that air in the pores affects the sound speed through the elastic moduli K and μ and through the density ρ of the sample.

Other than room temperature sound velocity measurements, there have not been many acoustic measurements in aerogels. de Goer *et al.* measured the internal friction and variation of sound velocity with temperature between 60 mK and 10 K[1.10]. A resonant bar method was used in this experiment so the frequency was very low (about 3 kHz). Figures 10 and 11 are their experimental results. In dense aerogels, the internal friction (essentially the attenuation of a sound wave) shows a plateau from 60 mK to 5 K and the sound velocity exhibits a logarithmic dependence in the temperature range of 70 mK to 1 K.

From the acoustic data above, it can be deduced that the number of TLS in aerogels is about same order of magnitude as that in bulk SiO_2. Therefore, the contribution of TLS to the specific heat of aerogels can be neglected since, from Fig. 4, the specific heat in aerogels is much bigger than that of bulk SiO_2. Moveover, because all the specific heat data is far below the Debye specific heat calculated from the sound velocities, some modes of vibration are missing or modified in aerogels. Two types of excitations have been suggested[1.8]: propagating low frequency phonons and localized modes but, since information

on low temperature excitations is very limited, there is not yet a good model.
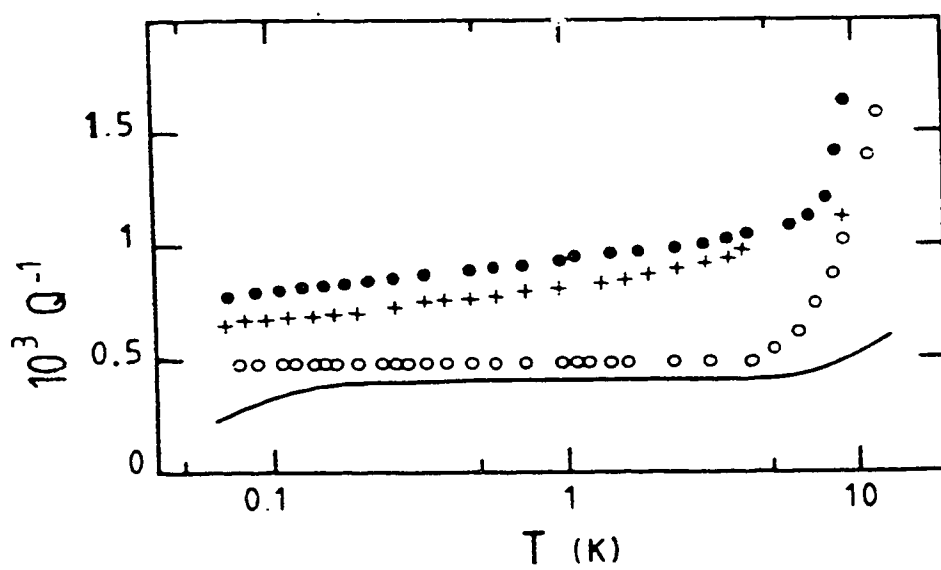
Fig. 10 Internal friction Q^{-1} of silica aerogels. ●: 0.87 g/cm³, ○: 0.27 g/cm³, +: 0.36 g/cm³,

solid line: Bulk α-SiO₂[1.10]
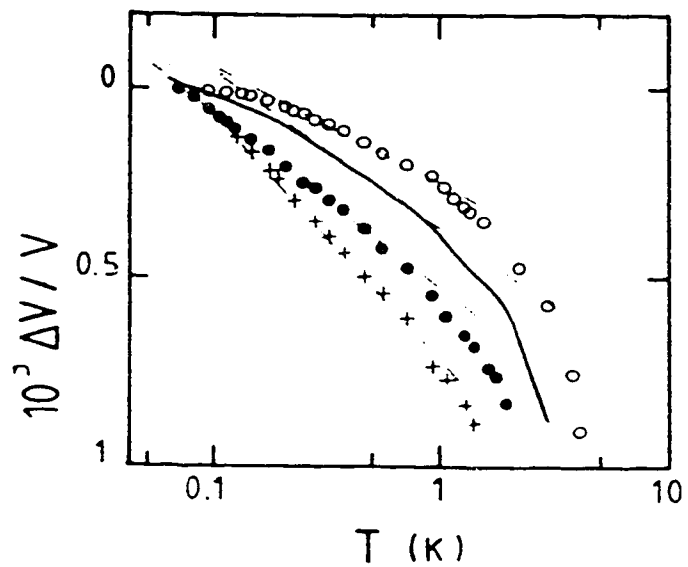
Fig. 11 Relative variation of sound velocity of SiO_2 aerogels. ●: 0.87 g/cm³, o: 0.27 g/cm³,

+: 0.36 g/cm³, solid line: Bulk α-SiO_2; broken lines: logarithmic regimes[1,10]

Chapter 4   **EXPERIMENTAL METHODS**

§4.1   Production of Aerogels

The making of aerogel starts with a sol-gel conversion by a catalysed chemical reaction of TMOS ($Si(OCH_3)_4$) and distilled water in methanol. To complete the process without shrinkage and collapse, the solvent is then removed hypercritically, i.e. above the critical temperature and pressure of the methanol. The work in this thesis involves making silica aerogels on a laboratory scale using this hypercritical drying process, based on a "recipe" developed by Hrubesh at Lawrence Livermore National Laboratory (LLNL) and Moses Chan's group at Penn State University[4.1]. This starts with the preparation of a solution to produce the chemical reaction needed to make the SiO_2 gel:

$$Si(OCH_3)_4 + 2\ H_2O \text{ ---- } SiO_2 + 4\ CH_3OH. \qquad [15]$$
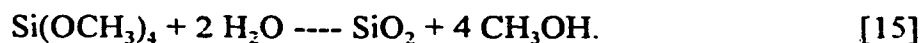
The resulting gel is then placed in an autoclave and heated. The pressure of the system then increases due to vaporization of the methanol. When it reaches 149.7 bar (2200 psi), a relief valve prevents it from increasing further. Heating is stopped when the system temperature reaches 270 °C, well above the critical point of methanol (Tc = 239.5°C, P = 80.9 bar). The methanol vapor is then released very slowly and the sample is cooled down while pumping out the residual methanol, finally producing the aerogel.

According to Chan's work[4.1], summarized in Tables 5 and 6, the molar ratio of water

to TMOS (Si(OCH$_3$)$_4$) must be exactly 2:1. To speed up the reaction, a small amount of

ammonium hydroxide ((NH$_4$)OH) should be used as a catalyst (Table 2). Methanol is added

to the solution in order to control the porosity of the final aerogel (Table 3).

NH$_4$OH solution	Gelation time	
	88% porosity	92% porosity
20ml H$_2$O + 0.04ml NH$_4$OH	30 min.	2 hr.
20ml H$_2$O + 0.03ml NH$_4$OH		overnight
20ml H$_2$O + 0.02ml NH$_4$OH	overnight	4 days
pure H$_2$O without NH$_4$OH		more than 4 weeks

Table 2. The gelation time and the concentration of the NH$_4$OH solution

TMOS	NH$_4$OH solution	Methanol	Porosity
3 ml	0.73 ml	1 ml	88%
3 ml	0.73 ml	1.8 ml	90%
3 ml	0.73 ml	3 ml	92%
3 ml	0.73 ml	7.3 ml	95%

Table 3. The solutions and final porosities

4.1.1. Making of aerogel

The whole aerogel making process can be divided into two parts.

4.1.1A. Gelation process

This process involves the chemical reaction [15] mentioned above. The solution for this chemical reaction is prepared based on the recipe of Hrubesh and of Chan in following steps:

1>. Add 0.4 ml NH_4OH (NH_4: 28-30%) to 200 ml distilled water to make the NH_4OH solution.

2>. Add 0.73 ml NH_4OH solution to the correct amount of methanol (98%) to produce the desired porosity and mix it well.

3>. Add 3 ml TMOS (98%) to the solution made in step 2 and mix it well, producing the gel solution.

4>. Pour the gel solution into a small glass vial 1.27 cm in diameter and 2.9 cm in height. Place the vial into a beaker filled with methanol, then cover the beaker with parafilm. The reason for doing this is to avoid drying the gel which would cause shrinkage at its surface.

5>. Leave it there to gel. In the case where the most basic NH_4OH solution was used, the least porous gel (86% with 0.5 ml methanol in the gel solution) gelled in less than 30 min. For the most porous gel (98% with 21 ml methanol), it took 4 days to gel. It is better to allow one or two extra days for aging the gels.

After the solution gelled, the vial was removed from the beaker and put into a stainless steel cell. The cell was filled with methanol and sealed and placed in the autoclave.

In order to achieve hypercritical conditions, a system was designed and built as shown in Fig. 12. The system includes five high pressure valves, since 149.7 bar (2200 psi) of pressure is required. For the same reason the volume of the system should be as small as possible. Therefore, 1/16" stainless steel tubing was used. The high pressure needle valve in this system is used to slowly release the methanol. Valve V_1 is used when evacuating the system, because the needle valve can't be completely shut off. The relief valve is used to control the pressure in the system. For methanol, it is set to limit the pressure to 149.7 bar (2200 psi). The capacitive pressure gauge is used to monitor the pressure in the system. A roughing pump connected to the system by valve V_4 does the pumping.

The gel sample is placed in a stainless steel sample cell 1.53 cm in diameter and 3.27 cm in height which is sealed with a copper gasket and connected to the system through the valve V_5. The cell is placed in an autoclave whose temperature is measured with a thermocouple and controlled by a digital temperature controller.

It is not possible to reach a pressure of 149.7 bar (2200 psi) in this system simply by heating the methanol in the cell because there is a comparatively large dead volume in the gauge. Therefore the rest of the system was filled with methanol: first, the system was pumped while the valves V_1, V_3, V_5 and the needle valve were closed and V_2 and V_4 open.
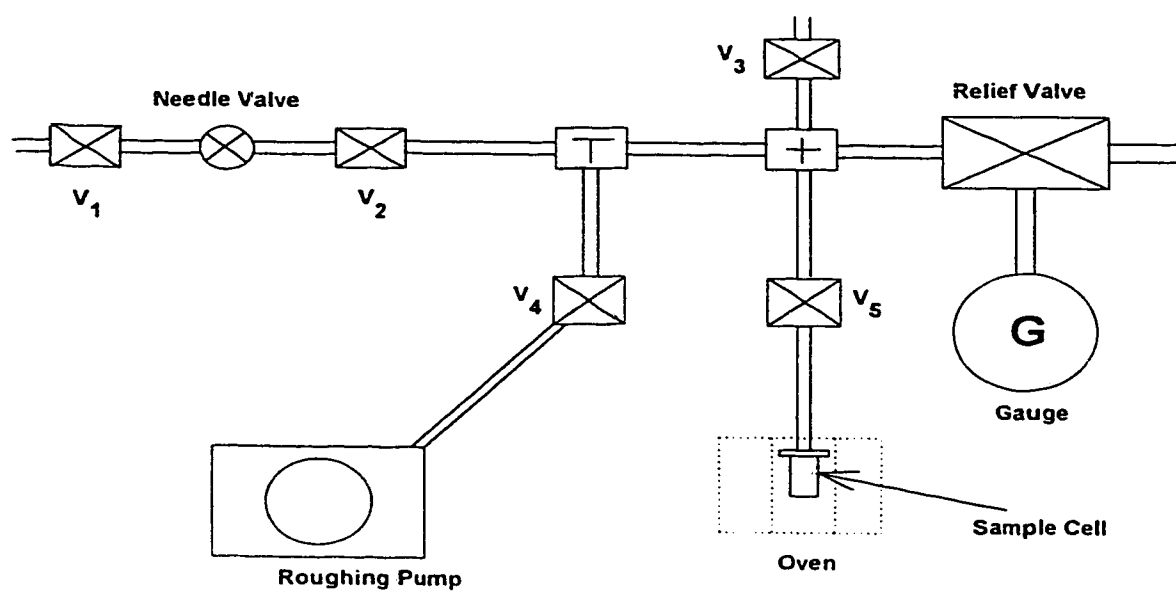
Fig. 12 The aerogel making system

After the system reached certain pressure, say 70 mTorr, V_4 was closed and the vacuum pump turned off. The capillary connected to the system by valve V_3 was placed in a beaker filled with methanol and V_3 opened, sucking the methanol into the system, including the cell (by opening V_5). Once the system was filled, V_3 and V_5 were closed. When the system was filled with methanol a much higher pressure could be built up. This completed the first step in making aerogels and was followed by the 2nd step, the hypercritical drying process.

4.1.1B. Hypercritical drying process

This process can be divided into 3 steps.

1>.   Heating

The temperature controller was programmed to have the heating and cooling cycle shown in Fig. 13. At first, it sat at 21 °C for a minute and then rose to 220 °C at a ramp rate of 1 °C/min. Secondly, the temperature ramped more slowly to 270 C at a rate of 0.5 °C/min. After sitting at 270 °C for 210 minutes, during which time the degassing (removal of the high pressure methanol through the needle valve) occurred, it was cooled to 20 °C in 120 minutes. The whole process took about 13 hrs.

2>.   Degassing
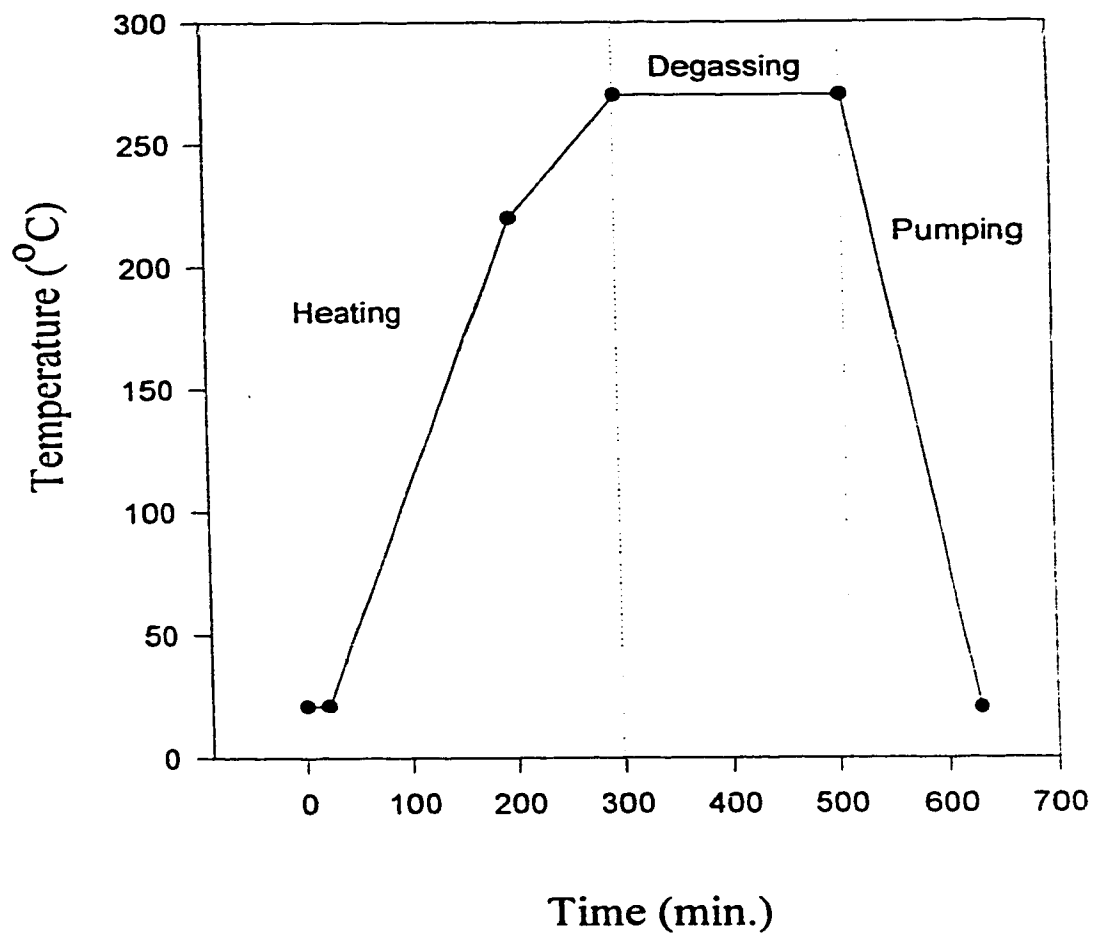
Fig. 13 The temperature cycle of the autoclave

Degassing was done once the system reached 270 °C and 149.7 bar (2200 psi). Valve V_1 and the needle valve were opened gradually to let the methanol out at the desired rate. For low porosity (< 92%) gels, the rate was less than 1.7 bar/min (25 psi/min), but for high porosity gels (> 94%), it could be about 2.0-2.4 bar/min (30-35 psi/min). Faster rates resulted in cracking and shrinkage of the aerogel.

This part is the hardest part in the whole process. On one hand, the degassing rate should be very slow because of the limited permeability of the aerogel. If the rate is too fast, the methanol vapor cannot escape from the aerogel quickly enough and a large pressure difference will build up causing the delicate structure to collapse. On the other hand, because the degassing rate decreases as the the system pressure drops, great care and experience is needed to adjust the needle valve, especially when the system is full of methanol.

3>.   Cooling and Pumping

At the end of the degassing, the system is at atmospheric pressure. The cooling and pumping procedure is to close V_1 and open V_4, turn on the vacuum pump to remove the residual methanol and let the system cool to room temperature.

A nice piece of aerogel can be made if the degassing rate is correct and degassing goes smoothly. If the rate is too fast, there are lots of cracks in the aerogel samples. Sometimes the methanol couldn't be removed easily because of silica dust left in the needle valve from

the previous run. This could cause the methanol to burst out suddenly or stop coming out at other times, resulting in cracks in the aerogel samples. The handling of the needle valve turned out to be extremely difficult.

§ 4.2   Cryogenics

4.2.1. The displex

Ultrasonic measurements were made in the temperature range from room temperature to 14 K using a CTI closed cycle helium refrigerator, referred to as the displex. The displex can run continuously which is necessary since one scan usually took about 3 days. The cooling power is very stable for a given temperature, allowing temperature control within 0.02 K.

The displex consists of a refrigerator and a chamber, which are connected as shown in Fig. 14. The refrigerator uses a compressor to provide the high pressure helium gas needed to operate and has two cooling stages. The first stage cools to about 75 K while the second reaches about 10 K. Below the first stage there is a hexagonal base with 6 vacuum feedthroughs: 2 coaxial connectors for ultrasonic signals, 2 electrical connectors for thermometry and temperature control (10 pin feedthroughs from Oxford Instruments), one gas fill line and a vacuum pump port. A stainless steel vacuum chamber surrounds the
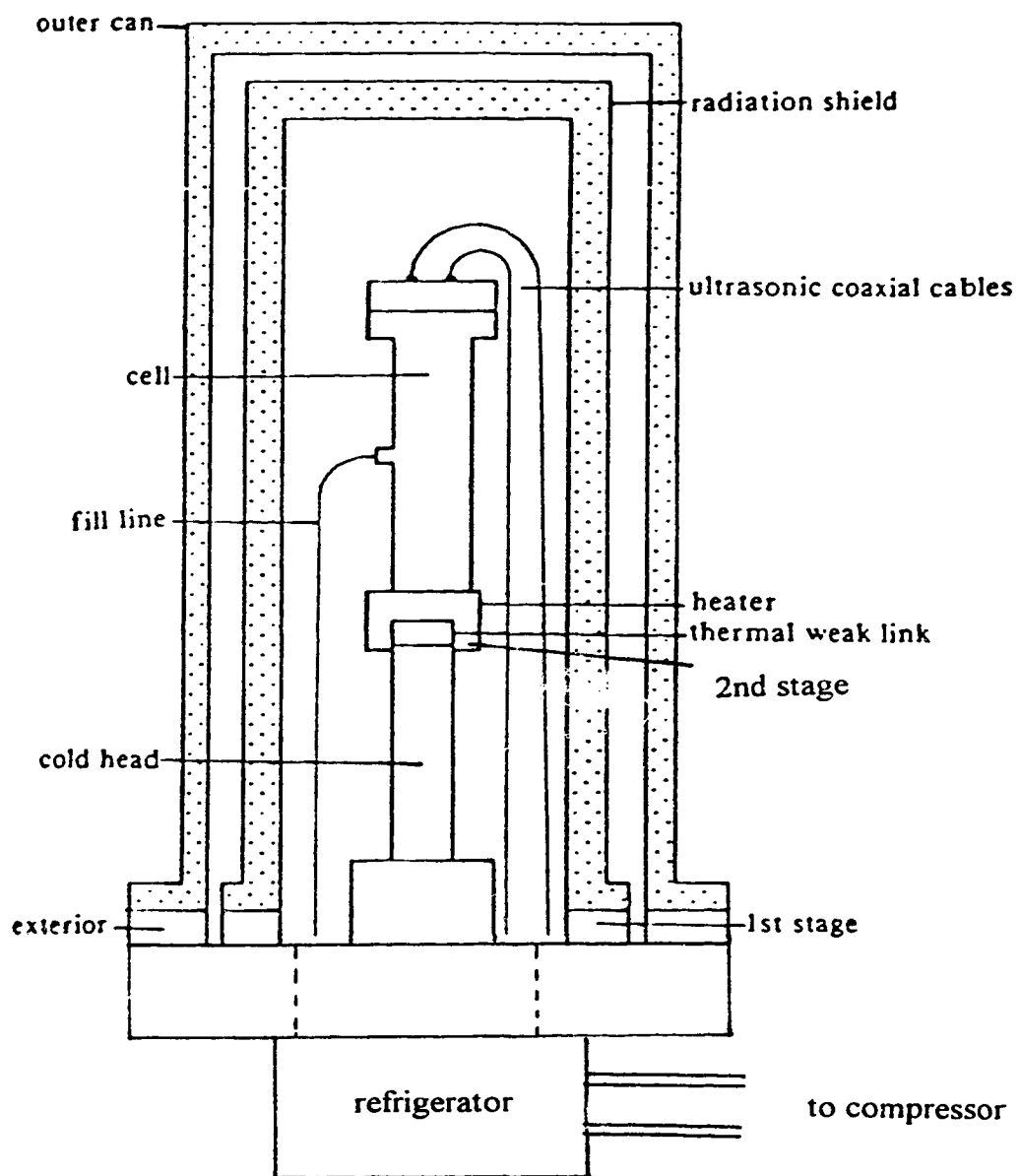
Fig. 14 The displex

refrigerator and is sealed to the base by a rubber O-ring and eight Allen screws. To control the temperature, a heater is placed on the second stage close to the sample cell.

The cold head of the refrigerator consists of a stainless steel tube with the first cooling stage, a round copper plate with 5 electrical and fill line connectors mounted on it, about half way up. The second stage is a flat, inch and a half diameter disk at the top. It has eight holes drilled near the circumference to allow attachment of various shaped heaters and cells. The second stage has a copper lid machined to just fit over it with a heater clamped around the side of the lid. The copper lid is connected to the second stage by a brass thermal weak link. Without the weak link temperature control is difficult, because of the temperature fluctuations which occur with every compressor stroke, several times per second. If the second stage is mounted directly on the top of the cold head, these fluctuations affect the temperature control. The weak link, which is machined in the shape of a thin cylinder sitting on a round disk the same size as the top of the cold head, provides a long thermal response time to minimize the effects of the temperature fluctuations.

The experimental cell sits on top of the copper lid, right above the second stage and must be thermally isolated from the exterior. Therefore, after the vacuum can is in place, the chamber is evacuated by a roughing pump to about 100 mTorr. During operation the cold head itself acts as a cryopump to further reduce the pressure and prevent heat exchange with exterior. Heating via blackbody radiation is reduced by a copper radiation shield which is fastened to the first stage by 6 Allen screws.

The other main heat loads on the displex are the electronic leads and the gas fill line. All electronic leads, for the heater, the thermometer and the ultrasonics, are fed in from the exterior by vacuum feedthroughs. Once inside the vacuum can, the leads are connected to another set of feedthroughs mounted on the first stage before continuing to the second stage. This thermal anchoring reduces the temperature gradient in the leads and thus the heat load on the cold head. Coaxial leads are used for the ultrasonic signal, even inside the displex, to avoid high frequency noise. These cables are a large potential heat load. However, if these cables, at least those from first stage to the cell, are made from stainless steel, which has low thermal conductivity, the heat load will be greatly reduced. The gas fill line is a sixteenth inch stainless steel tube and extends from the exterior to the cell. With this tube thermally anchored to the first stage, the displex usually cools to about 12 K.

4.2.2. Thermometer and temperature control

The thermometer is a calibrated carbon glass resistor glued inside a copper disk. It is placed close to the sample, on the cell, which is therefore machined with a flat and smooth face to ensure good thermal contact. The thermometer is screwed onto this flat with a layer of vacuum grease. The thermometer has four leads: 2 for the current, 2 for measuring the resulting potential. The temperature of the thermometer is measured using a digital resistance bridge and temperature controller (Quantum Design 1802). The absolute accuracy of the bridge is better than 0.05%, which gives a negligible contribution to the error in the temperature measurement. Since the refrigerator cooling power cannot be controlled, heat

is needed to reach a temperature setpoint. With the 150 ohm heater, the temperature controller can supply a power up to about 18 watts. The bridge has two driver channels. One is linked to the input channel that measures the resistance of the thermometer and is used to control the temperature. The other can be used to supply a fixed output power to a heater on the first stage of the displex.

The bridge is controlled by a Zenith 386 computer which sends it a resistance set point, a feedback gain, and two time constants, one for the integrator (τ_I) and the other for the differentiator (τ_D). After receiving all these parameters, the bridge uses a standard PID (Proportional, Integral, Differential) algorithm to control the temperature. Besides sending the control parameters, the computer is also programmed to specify the range that the temperature may fluctuate around the setpoint. If the temperature stays within this range for thirty seconds, the cell temperature is considered stable and data are taken.

4.2.3. The cell

The sample is mounted within a copper cell attached to the copper lid on the second cooling stage by a screw threaded into a tapped hole in its base. The cell is made from oxygen free high conductivity (OFHC) copper, a very good thermal conductor, to maintain thermal equilibrium. It has two main parts: an outer jacket and an insert. The outer jacket is basically a cylinder 6.85 cm in height, with a 1.64 cm inner diameter and a 2.35 cm outer diameter. It also has a flange with 6 threaded holes near the circumference to attach the

insert. The insert is machined as a round top with the same diameter as the flange, 3.25 cm, and an attached sample support, as shown in Fig. 15. There are six holes drilled in the top to match those the flange. There is O-ring groove on the inside face of the top so that the insert can be sealed to the outer jacket by an indium O-ring.

The ultrasonic cables are connected to the electrodes on the sample holder through feedthroughs soldered into top of the cell insert. Inside the cell, the signal is transmitted to and from the transducers by thin gold wires.

There is a gas fill line to admit helium exchange gas into the cell for thermal contact. It is soldered into a small brass fitting on the wall of the cell. The fill line is a sixteenth inch stainless steel tube which is connected to an HIP taper seal fitting thermally anchored at the first cooling stage and then goes to a feedthrough on the hexagonal base.

§4.3   Ultrasonics

To study the acoustic properties of the aerogels, ultrasonic measurements are used. From these, not only could the actual sound velocity in aerogel be determined, but also the changes in sound velocity and attenuation with temperature.
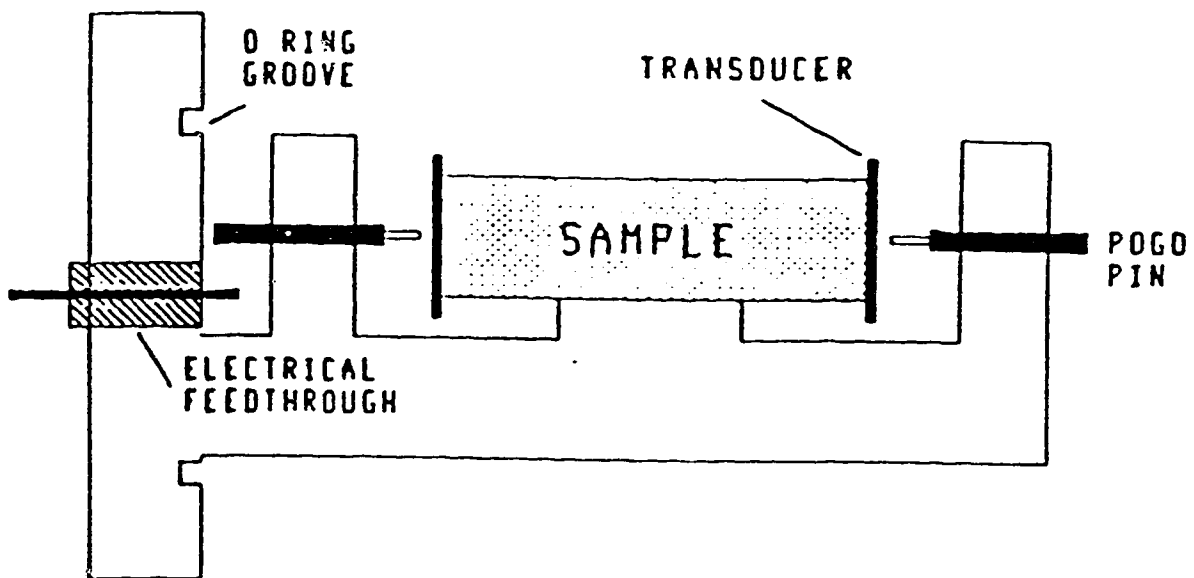
4.3.1. The ultrasonic system

Fig. 15 The cell

Most of the ultrasonic measurements involved the changes in velocity and attenuation with temperature. The temperature range covered was from room temperature down to 14 K. The frequencies used were in the range from 3 MHz to 18.5 MHz and both longitudinal and shear modes were used. The aerogels studied had porosities from 80% to 89.5%.

The ultrasonic system was designed to measure small changes in sound velocity and attenuation rather than absolute values. It has the following specifications:

Frequency range:	2 - 200 MHz
Receiver bandwidth:	2 MHz
Transmitter output power:	10 pW - 100 mW (pulsed)
Phase resolution:	1 mrad
Amplitude resolution:	0.005 dB
Linearity:	0.1 dB (over 10 dB range)
minimum pulse width:	1 µsec
maxmum pulse repetition rate:	4 kHz

The measurements use a pulse-echo method in which the sample is placed between two parallel transducers. The sound wave, either shear or longitudinal, is generated by one transducer and is transmitted to the other through the sample. It reflects from the receiving transducer due to the acoustic mismatch with the sample, producing an echo. Successive echoes can be seen when the attenuation is small. For aerogel, however, there are generally

only one or two echoes.

The sound velocity in the sample at some arbitrary reference temperature is

$$v_o = D / t_0,$$ [16]

where D is the sample length and t_0 is the transit time of the sound wave through the sample. The relative sound velocity is

$$\frac{v}{v_0} = \frac{D/(t+\Delta t_0)}{D/t_0} = \frac{t_0}{t_0+\Delta t}$$ [17]

where Δt is the change in transit time. Since

$$\Delta t = \Delta \Phi / 2\pi f,$$ [18]

where $\Delta \Phi$ is the change in phase with respect to its original value and f is the sound frequency, the relative velocity is

$$\frac{v}{v_0} = \frac{1}{1 + \frac{\Delta\Phi}{2\pi f t_0}}.$$

[19]

To determine either the change in sound speed or its absolute value, the transit time must be measured. The round-trip transit time is measured by comparing the arrival times of consecutive echoes. The sound velocity is then obtained by using equation [19], where t_0 is half of the round-trip transit time. Its absolute accuracy is about 1% because it is limited by the transducer bond which has its own sound speed and a finite thickness. There is no way to separate transit times through the bond from those in the sample. Furthermore, the absolute accuracy is limited by how well the effective sample length is known. For the aerogel samples used, for example, it is much worse than 1% since the sample lengths were so short that they were almost comparable to the thickness of the bonding layers.

The changes in sound speeds are too small to determine accurately by directly measuring the changes in transit time. Instead, the changes in the phase of the received signal are measured since they can be found very accurately by comparing to a reference signal. The changes in the sound velocity can be determined from the changes in phase $\Delta\Phi$ and the original velocity v_0, transit time t_0 and the frequency of the sound wave. In a typical case, for a frequency of 10 MHz, the resolution of the system for changes in sound velocity is a few parts per million.

The attenuation is the decrease in the pulse amplitude. However, this decrease is not just that in the aerogel sample if the boundary conditions are not good enough. As a matter of fact, it's very hard to have good boundary conditions. The bonds between the aerogel sample and the transducers have finite thicknesses and are very complicated. Moreover, the two transducers cannot be placed perfectly parallel. Therefore, what is really measured here are not absolute values but rather the changes in attenuation when, for example, the temperature is changed or gas is added.

There are two ways to determine the signal amplitude. One is from the phase-detected signal. The total amplitude is the root square sum of the in-phase (X) and quadrature (Y) components measured by the ultrasonic system. The other method is just a measurement of the amplitude of the signal before it is phase detected.

The attenuation measurements require a detectable sound pulse be transmitted through the sample. In the case of the LLNL aerogel the signal was quite decent throught the whole temperature range from room temperature to 14 K. In the aerogels made here, almost no signal got through between roughly 100 K and 70 K. All the aerogels attenuated the ultrasonic signal more than vycor or other glasses so there were no successive echoes and high frequencies (odd harmonics of the transducers) could not be used.

The ultrasonic system is shown in Fig. 16. Basically, there are three parts: sending, receiving and signal processing. The sending part consists of a radio frequency (RF) signal
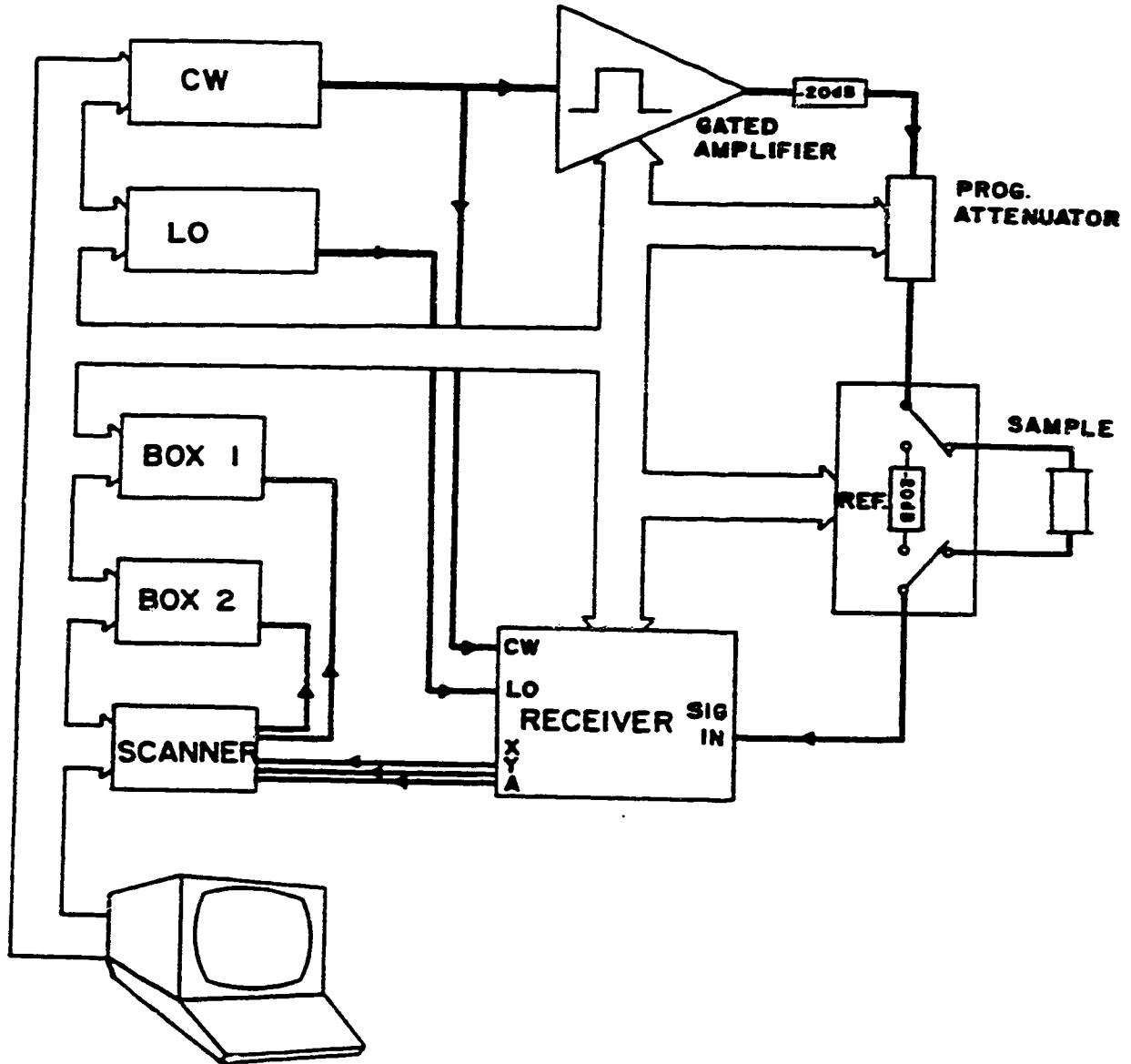
Fig. 16 Schematic drawing of the ultrasonic system

generator, gated amplifier and programmable attenuator which provides RF pulse which is sent to the sample as well as the reference signal. The receiving part, a heterodyne system, has a local oscillator (LO) which is mixed with the received RF signal from the sample. The resulting echos are phase and amplitude detected. The pulse trains then arrive in the signal processing part which includes two boxcars, two multimeters and a scanner. The signals are averaged by the boxcar gated integrator before further processing by the computer. Finally the computer calculates the changes in sound speed and attenuation. The entire system is computer controlled.

The same measurements were made on a reference sample (a fixed attenuator), as well as on the experimental sample, in order to eliminate long term drift of the amplifiers in the system. This drift can have an effect on the final results since most of the scans take at least two days to complete. This drift is mainly due to daily fluctuations in the room temperature. The real changes are obtained by subtracting the drift data from the data from the sample.

4.3.2. The heterodyne system

The heterodyne system converts ultrasonic signals at different frequencies to the intermediate frequency (IF) of 155 MHz, the working frequency of the phase detector. Fig. 17[4.2] shows the heterodyne system. Basically the RF signal of frequency f, generated by CW, is split into two. One part mixes with the local oscillator (LO) signal, which is always at a frequency 155+f MHz, yielding a reference signal at the IF of 155 MHz as well as a signal at
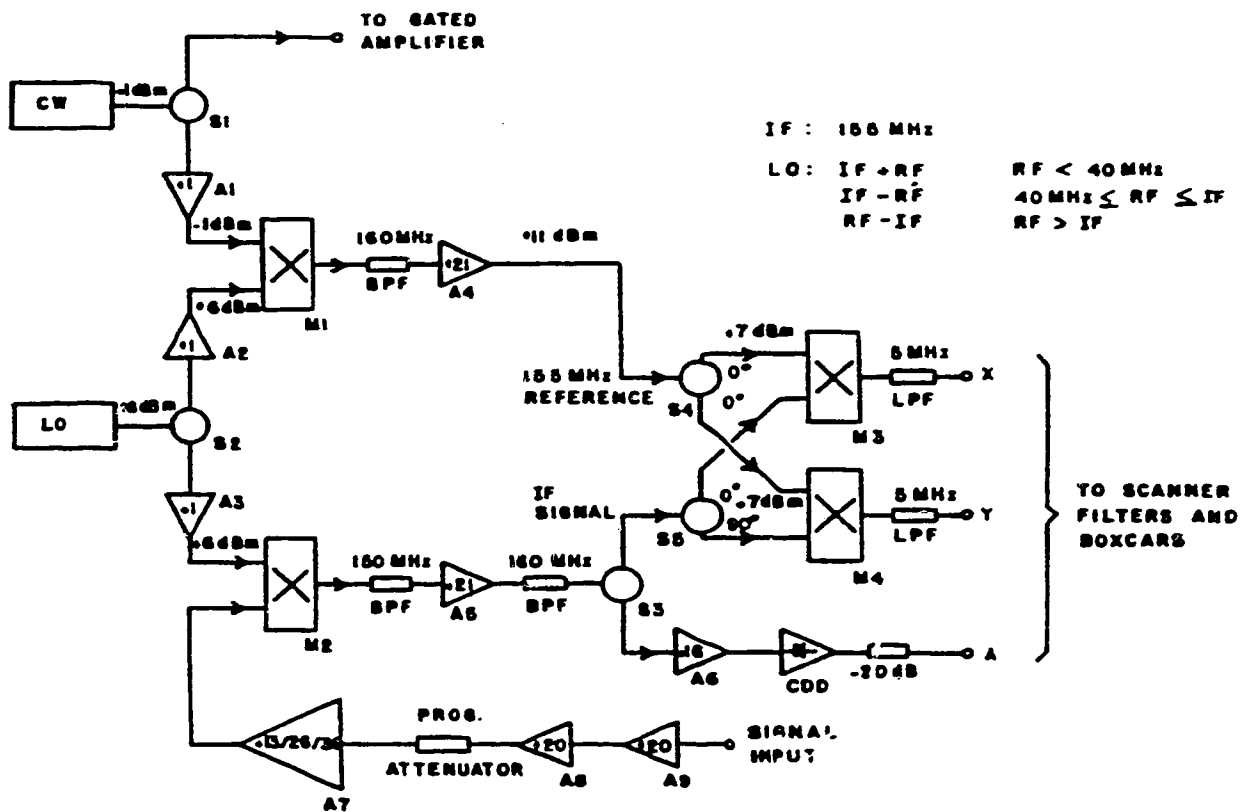
Fig. 17 Schematic drawing of the heterodyne receiver

155+2f MHz. The other part goes through the sample and then mixes with the LO signal,

resulting in sample signals at the same two frequencies. To get rid of the signals at 155+f

MHz, three bandpass filters are used. The center frequency of one is 150 MHz (BPF 1) and

of the other two is 160 MHz (BPF 2, 3). The 155 MHz reference signal goes to a splitter

"S4". Meanwhile, the signal from the sample reaches "S3" where it is split into a "Z

component", which is the rectified IF signal from the sample, and a part which is sent to "S5",

a phase shifting splitter which outputs an in-phase signal and a 90° phase shifted signal.

These are then mixed with the reference to yield DC (0 Hz) signals as well as high frequency

(310 MHz) signals which are later removed by low pass filters. The DC signal which was

not phase shifted is the "X component" while the quadrature signal (the one phase shifted by

90°) is the "Y component". From the X and Y components of the output pulse, the phase can

be determined by:

$$\Phi = \tan^{-1}(Y/X) \qquad [20]$$

and the amplitude is found from either the root square sum of the X and Y components or

from the amplitude of the Z component.

Fig. 18 shows typical output pulses from the heterodyne system. The input pulse on

the top trace ("RF pulse into sample") is called the "main bang". It can usually also be seen

on the receiver output because of electrical cross-talk between the incoming and outgoing

paths. The pulses on the "receiver output to boxcar" traces are the signal of interest, the first

RF PULSE
INTO
SAMPLE

SIGNAL
FROM
SAMPLE

RECEIVER
OUTPUT
TO
BOXCARS

A

X
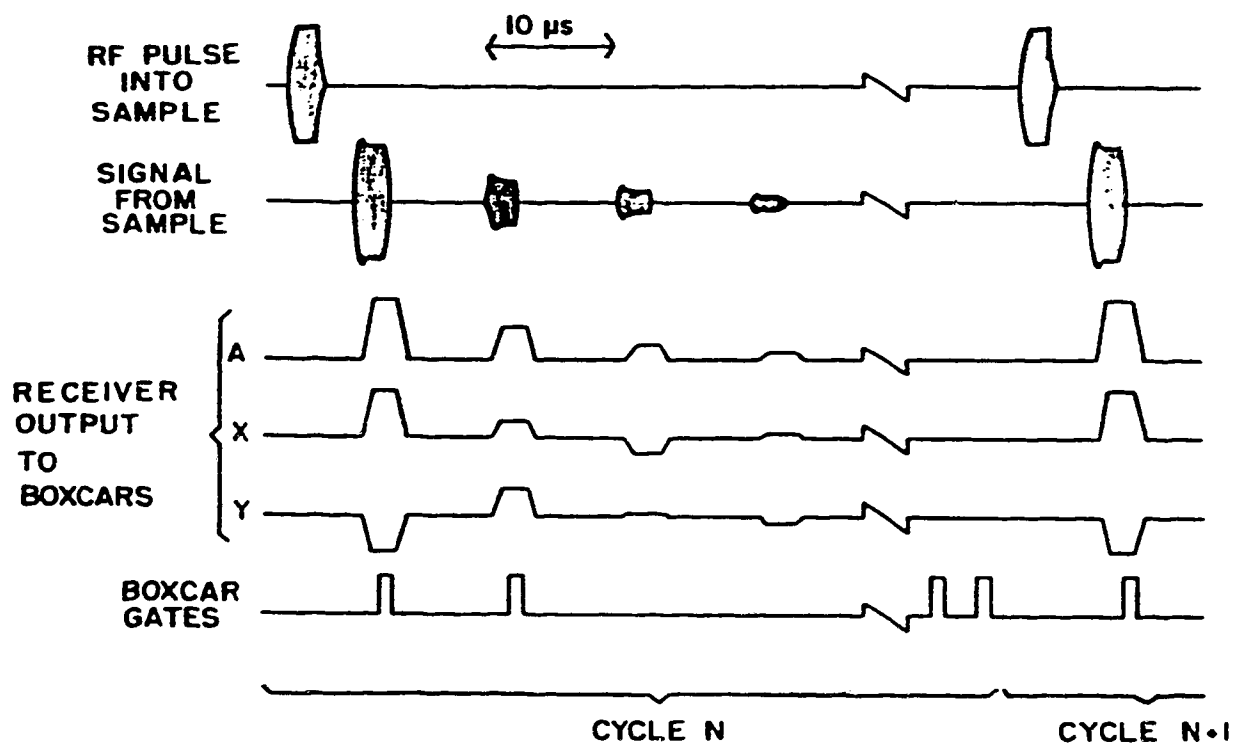
Y

BOXCAR
GATES

10 µs

CYCLE N

CYCLE N+1

Fig. 18 Signal traces in various parts of the system

being received after one pass through the sample and the others are subsequent echoes. The gates of the boxcars are set on these pulses. More than one echo is rarely seen in the case of aerogels.

The transit time t_0 for aerogel samples is usually measured from the main bang to the pulse of interest since the main bang shows when the pulse was generated and the other pulse arrives after passing through the sample once.

§ 4.4   Sample Preparation

4.4.1. Aerogel

The two sides of aerogel samples for ultrasonic measurements should be cut to ensure that the transducers are parallel. In addition, the samples, especially those cut from aerogels made in our lab, must be very thin to get acceptable signals, about 2 mm or less. Grinding to this size is almost impossible since aerogels are very fragile. A better method is to cut the samples on a high speed (40000 rpm) wafer wheel. An aerogel piece was taken from the vial it was made in and glued to a holder using epoxy. Two parallel cuts were made to make sure the sides of the sample to which transducers were to be attached were parallel. It is difficult to cut aerogels very precisely since they are both brittle and compressible. This also makes it hard to determine the length of a sample with great accuracy. After cutting, the surfaces

of the samples look quite smooth. There was definitely dust on the surfaces but there is no obvious way to remove it since a solvent would destroy them.

4.4.2. Transducers

The transducers used were lithium niobate (LiNbO$_3$) longitudinal transducers with a fundamental frequency of 20 MHz. They have higher efficiency than quartz transducers and can often be used over a frequency range from about 10% of their fundamental up to 20% above it, as well as at odd harmonics. The great advantage of using transducers with a high fundamental frequency is that it provides a wider frequency range and therefore a better chance of getting good signals. However, the higher the fundamental frequency, the thinner the transducer and 28 MHz transducers are already uncomfortably fragile. Therefore, all data in this thesis was taken using 20 MHz transducers, unless otherwise noted.

The transducers were cut to the desired size, about 4 mm × 8 mm, with a string saw and then cleaned with acetone and gently wiped with Q-tips. Ultrasonic cleaning is not recommended, since it damages the gold electrodes plated on the transducers. Gold wires are soldered onto the transducers as electrical leads before bonding them onto the aerogel sample. These wires must be strong enough not to break when they are soldered onto the transducers but flexible enough so that they do not pull on the transducers and bonds and damage the samples. Soldering of the wires must be done with great care since the transducers are very fragile. A very hot soldering iron or too much pressure will crack the transducers. Only a

little solder and flux are used. Experience is also necessary. Finally the connections between the wires and the transducers are checked with a multimeter and the transducers are cleaned again in the way described above.

4.4.3. Bonds

Making bonds between the transducers and the aerogel sample was the most difficult problem in this work. Liquids, such as the silicone oil often used for ultrasonic bonds, damage the aerogel, even turn it into powder. In an attempt to block the absorption into the pores, an indium layer was evaporated onto both surfaces of an aerogel sample. However, even 10 kÅ thick indium layers did not stop the absorption. Although most epoxies also damage the aerogels, some seem to work better with only minor damage. One that is particularly easy to use is a silica powder-filled epoxy, TRA-BOND 2151. Damage appears to be limited to a thin surface layer and it forms reliable bonds. It takes half a day to cure at room temperature.

For this work, all transducers were bonded to the aerogel samples with the TRA-BOND epoxy. The transducers were pressed carefully onto the aerogel with a flat headed wooden stick after they were aligned so that their active areas overlapped. Samples were left overnight to let the bonds cure. The whole sample, aerogel with transducers, was then mounted on the sample holder of the cell and the transducer leads connected.

§ 4.5   Ultrasonic Measurements

The ultrasonic measurements of the changes in sound velocity and attenuation were made from room temperature to 14 K at as many frequencies as possible. For aerogels, the frequency range, from about 3 MHz to 18.5 MHz, was limited not only by the fundamental frequency of our transducers but also by the aerogel itself. To get a decent signal the thickness of the samples had to be as thin as possible since aerogels attenuate the sound wave a lot. However, they couldn't be too thin; otherwise, the signal would overlap the main bang. A transit time of at least 4 μs is required. A sample thickness of around 2.0 mm turned out to be the best compromise.

After the sample was sealed into the cell, the leads hooked up and the radiation shield and vacuum can installed, the air in the cell was evacuated, otherwise air would liquify in the pores at low temperature. Once evacuated, the only thermal connection between the sample and the cell was through the four very thin leads from the transducers. As a result, the temperature measured was not the temperature of the sample. In order to solve this problem, a thermal exchange gas was admitted to the cell. Helium was chosen due to its very low boiling point (4 K). In order to ensure that there was as little air as possible in the cell, it was first pumped by a turbo-molecular pump for about 15 minutes. Then the pump was disconnected and the cell filled with about 2 atmospheres of high purity helium (see Fig. 19). The cell was pumped again and the same flushing procedure repeated twice. Finally, about 1 atmosphere of helium was left in the cell as exchange gas. It was in the pores of the aerogel
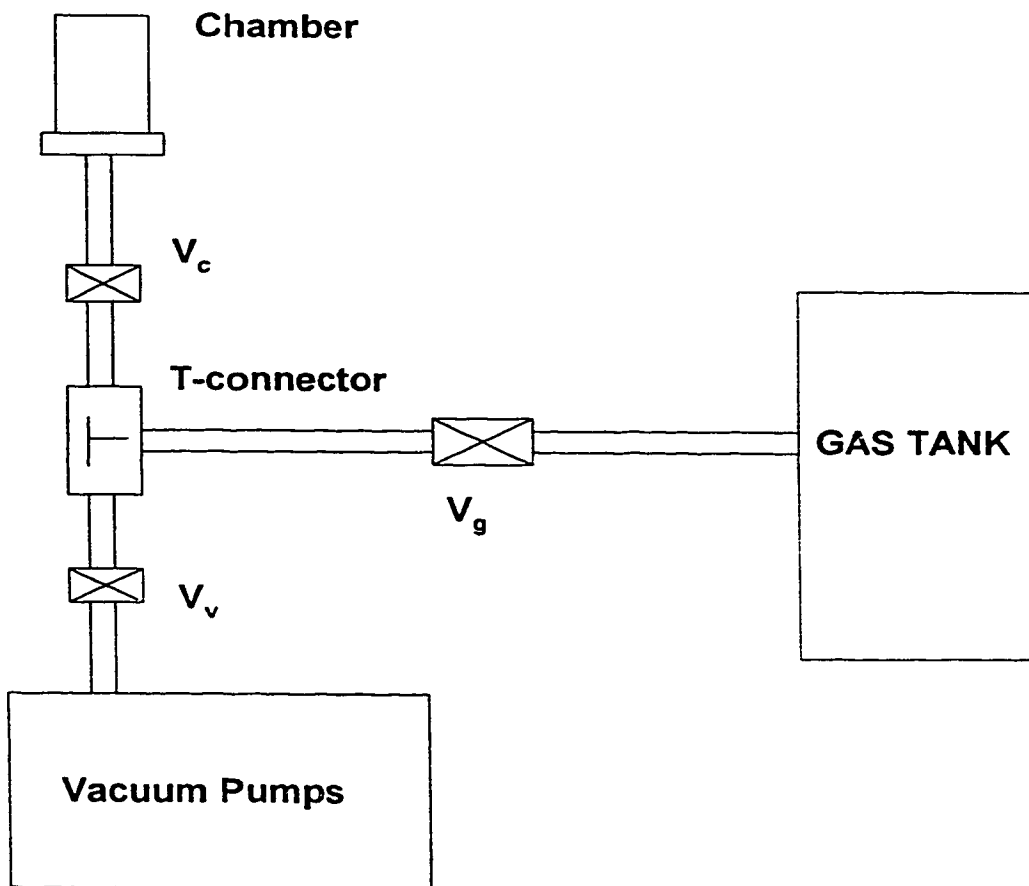
Fig. 19 The exchange gas handling system

samples while the ultrasound data were taken. However, it was thought its effect could be ignored since its density and its modulus contribution were much smaller than those of the aerogel, and its contribution to the attenuation was also small.

Before taking ultrasonic data, a preview of the whole scan was necessary for three reasons. The first was to decide at which frequencies the signal was good enough for data to be taken. The second reason was to have a rough idea about the size of the signal throughout the whole temperature range so that the pulse amplitude could be adjusted in order to stay in the linear range of the ultrasonic system. The third reason was to find the boxcar gate position for the entire temperature range. This was very important for aerogels, since the sound velocity changed considerably with temperature. Data were taken every 10 K in this pre-scan.

All ultrasonic data were taken by computer. Between room temperature and around 100 K, data were taken every 3 K. From around 100 K to 50 K, they are taken every 0.5 K, and from around 50 K down to 14 K, every 3 K again. Taking closely spaced data around liquid nitrogen temperature was necessary to continuously track the change of phase with the temperature since the velocity varied rapidly in this temperature range.

Chapter 5   RESULTS

§5.1   Aerogels Produced

By using the hypercritical drying process, a number of pieces of aerogel were made as summarized in Table 4:

Sample	#8	#21	#29	#27	#4	#9	#15
ρ_p (g/cm³)	0.312	0.287	0.253	0.235	0.124	0.066	0.042
ϕ (%)	85.8	86.9	88.4	89.3	94.3	97.0	98.1
CH_3OH	0.5ml	0.75ml	1.6ml	1.8ml	7.3ml	14ml	21ml

Table 4. The density and porosity of aerogels made in our lab

The density method was used to measure the density ρ_p of each aerogel as well as its porosity $\phi = 1 - \rho_p/\rho_s$. Here ρ_s is the density of bulk silica, 2.19 g/cm³. From Table 4, our results match those of Chan's group shown in Table 3 quite well.

All these samples were bluish, quite transparent and very light. The higher porosity ones were more flexible than the less porous ones. When released after squeezing them, they bounced back. When dropped, they bounced with a clear metallic ring.

§ 5.2   Discussion on Production of The Aerogels

Using the one step method, aerogels of porosity from 87.0% to 98.1% could be prepared. The reason that only this range is accessible is that a porosity of 87% corresponds a starting solution with only 0.5 ml of methanol, which then gels so quickly that it can barely be mixed, while a porosity of 98.1% correponds to a solution with 21 ml methanol, in which case it takes more than 4 days to gel. The catalyst used here was the most basic NH_4OH solution in Table 2.

The most important parameter in the drying step was the degassing rate. It was about 1.5 bar/min (22 psi/min) for aerogels with 87.0% porosity and 2.2 bar/min (32 psi/min) for aerogels of 98.0% porosity. The choice of degassing rates was due to the porosity dependence of the permeability of the samples. Rates which were too fast resulted in lots of cracks while very slow rates were too time consuming. It was very important that the system be kept clean since dust and residual aerogel pieces can cause sudden bursts of methanol from the needle valve and corresponding pressure changes.

§5.3   Ultrasonic Velocity and Attenuation

Detailed ultrasonic measurements were made on several samples made here and on one made at LLNL. Longitudinal and transverse sound velocities were first measured at

room temperature. Information on these samples is given in Table 5 :

Sample #	$\rho(g/cm^3)$	ϕ (%)	L (mm)	v_l (m/s)	v_t (m/s)
21	0.287	87.0	1.5	279	165
29	0.254	88.5	1.0	234	156
~7	0.235	89.3	1.2	250	154
LLNL	0.360	84.5	2.9	598	363

Table 5 Sample properties

The sound velocities in this table have quite large uncertainties since the sample
lengths are small. With a microscope it can be estimated that about 10% of each sample is
affected by the epoxy bonds to the transducers. The uncertainty is the highest for the thinnest
sample #29.

The temperature dependence of the attenuation and velocity were measured while
cooling. Both longitudinal and transverse data were taken. Since the main interest was in the
changes in attenuation with temperature and the absolute values of attenuation couldn't be
determined from these measurements, the data curves in this chapter have been offset for
clarity (i.e. the "0" position is arbitrary). Figures 20 to 22 show the frequency dependence
of the attenuation of longitudinal waves in the LLNL sample and in samples 27 and 21. In
all samples, for both modes and at all frequencies, there is a large attenuation peak around 60
to 80 K. However, the attenuation peaks are much smaller in the sample made at LLNL, as
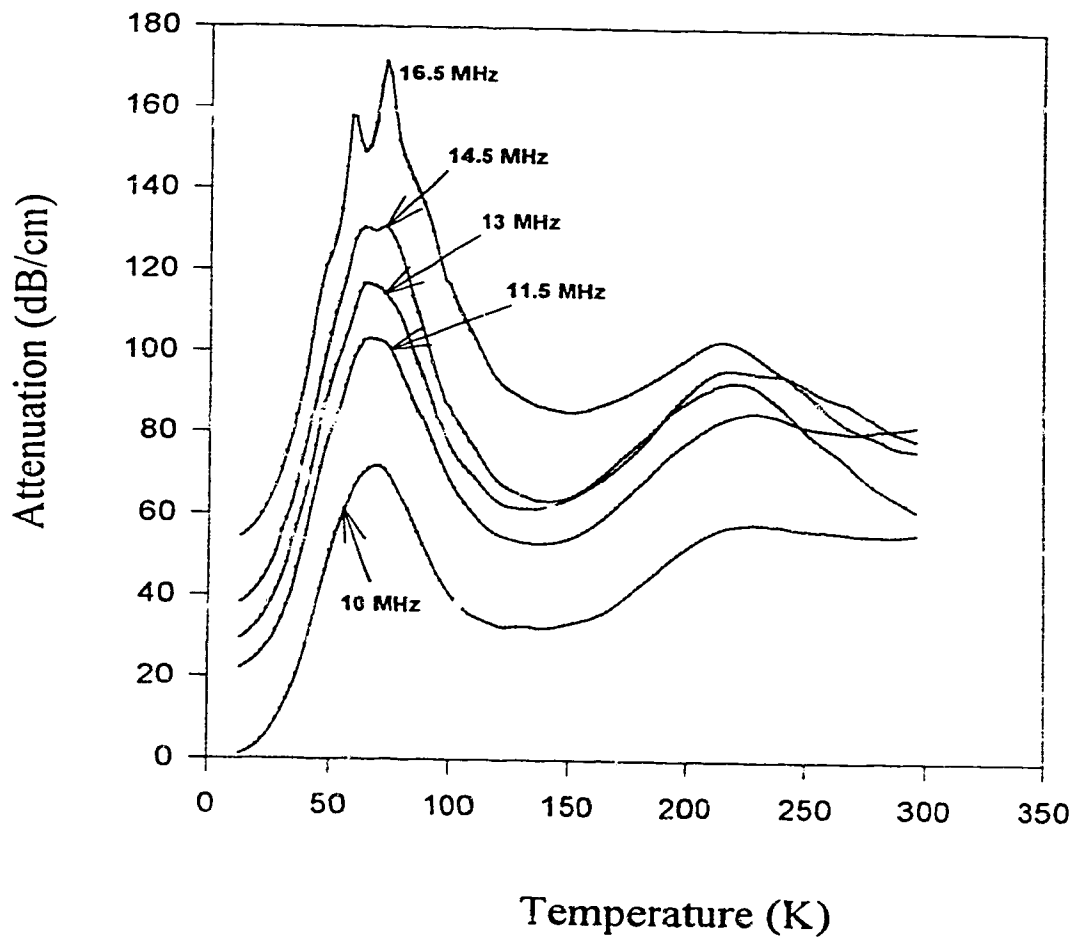
Fig. 20 Acoustic absorption of longitudinal waves in aerogel (LLNL, 0.360 g/cm³)

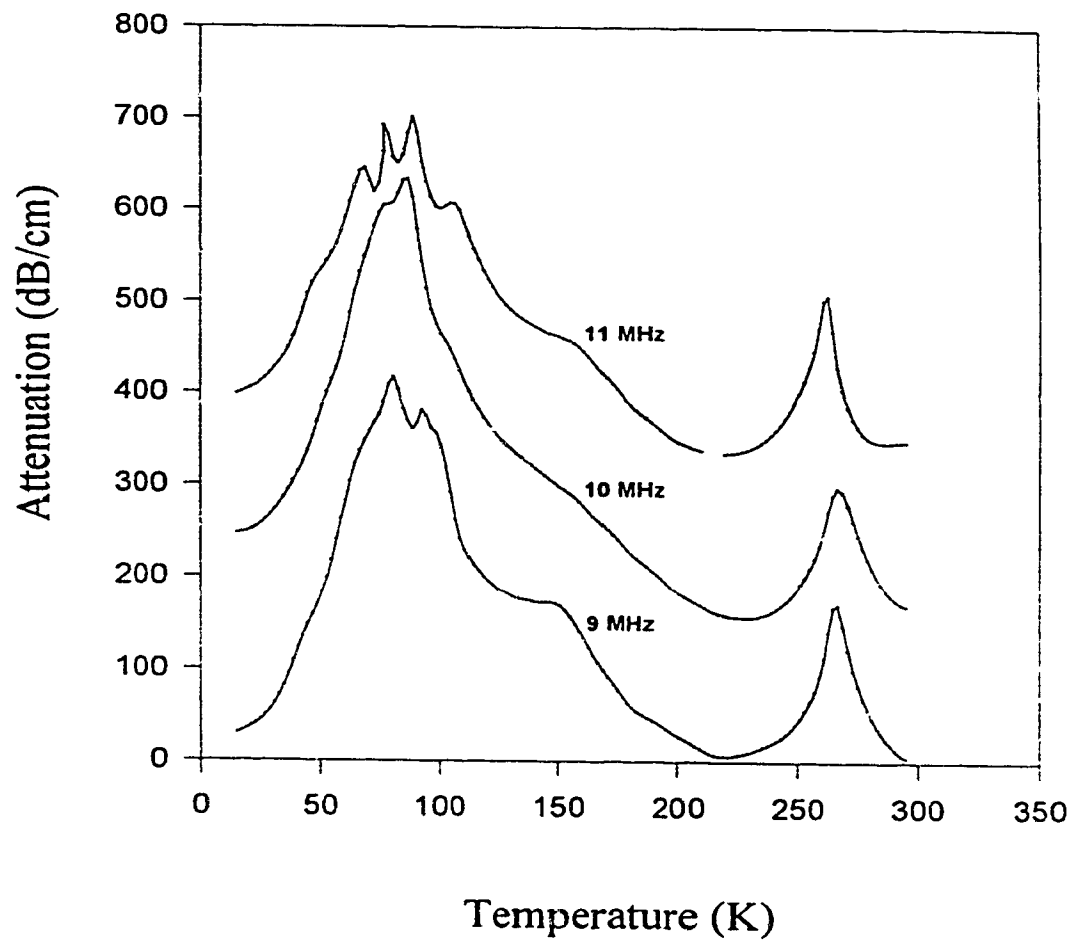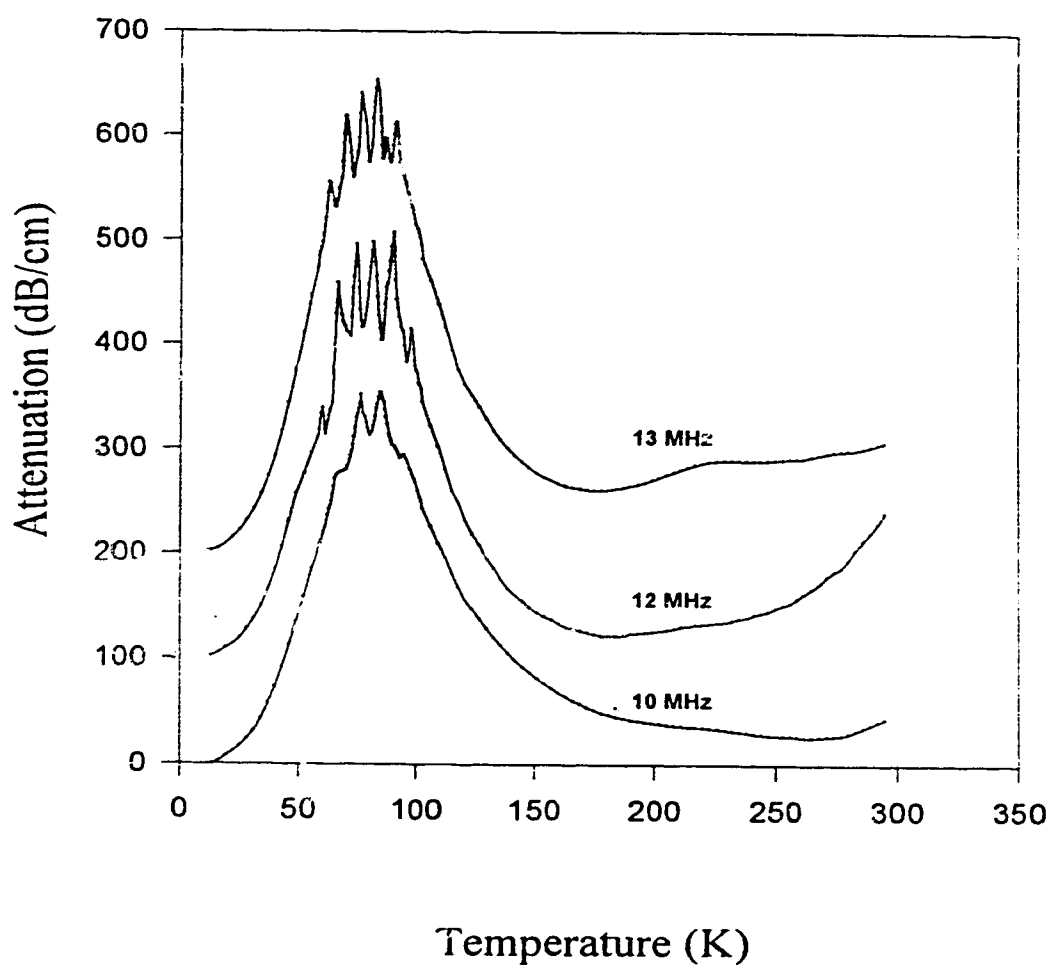Fig. 21 Acoustic absorption of longitudinal waves in aerogel (#27, 0.235g/cm³)

Fig. 22 Acoustic absorption of longitudinal waves in aerogel (#21, 0.287 g/cm³)

can be seen clearly from Fig. 23 which compares the 10 MHz attenuation in the three samples. Near some of the peaks the signals were below the linear range of the ultrasonic system, which resulted in spurious wiggles in the data. The LLNL sample, Fig. 20, covers the widest range of frequencies. The large peak below 150 K becomes larger as the frequency increases. The limited frequency range (10 to 16.5 MHz) and the distortion near the peak make it impossible to determine whether the peak position shifts with frequency. In the samples made here (shown in Figs. 21 and 22), the attenuations are larger and it is more difficult to see the frequency dependence of the attenuation peak because of the wiggles. Below 50K, however, it is clear that all the attenuations increase with frequency. The attenuations appear to be proportional to T^3, as shown in Fig. 24. For shear waves, data is only available at a few frequencies and Fig. 25 compares the attenuations in the three samples at similar frequencies..

In the samples made here, the density dependence of the of the attenuation is unclear, since the range of densities is actually quite small. However, Figs. 23 and 25 show that the highest density LLNL sample (0.360 g/cm^3) has much smaller attenuation for both longitudinal and shear waves.

The corresponding variations of sound velocity with respect to temperature are shown in Figs. 26 - 29. As for the attenuation, the changes of sound velocity with temperature are the main interest, even though the absolute values can be measured to within 5 or 10%. The figures plot the changes in sound velocity ($\Delta v/v_0$), i.e. the fractional change with respect to the sound velocity v_0 at some reference temperature. Again, data at different frequencies or
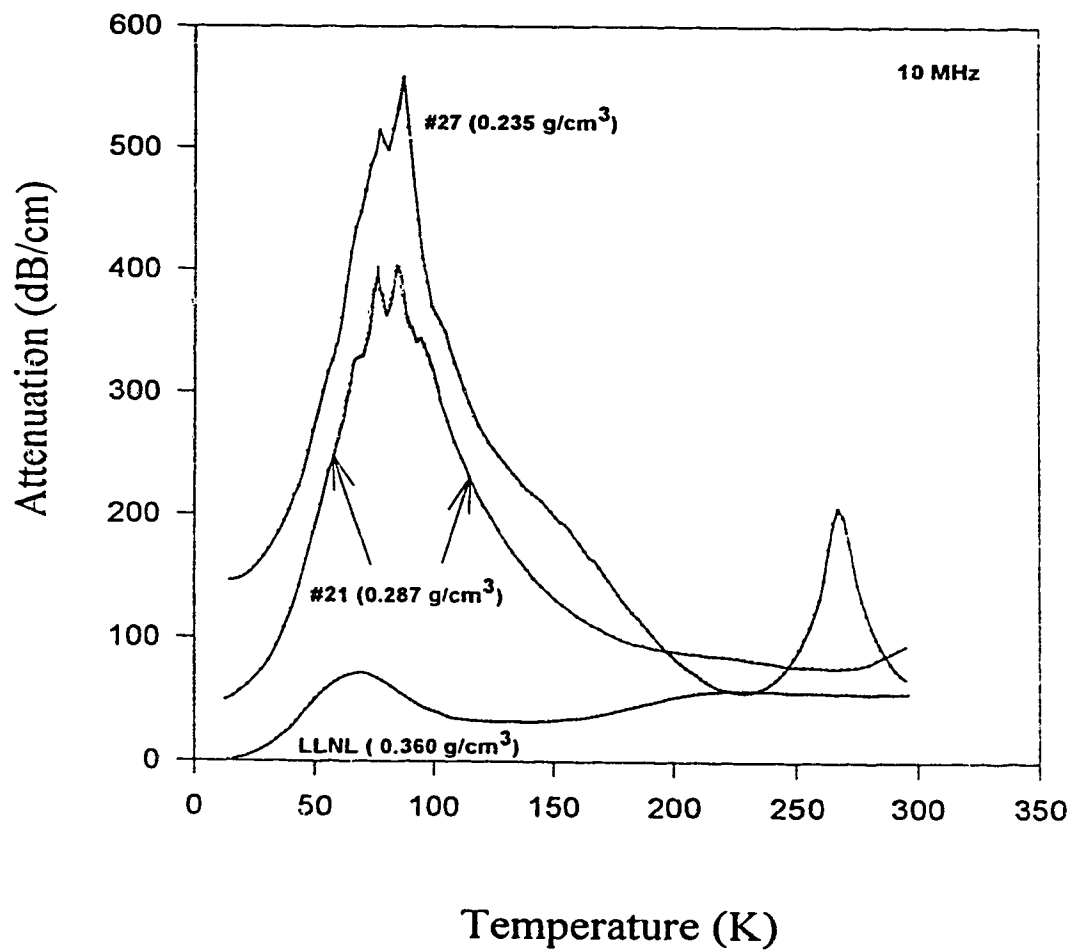
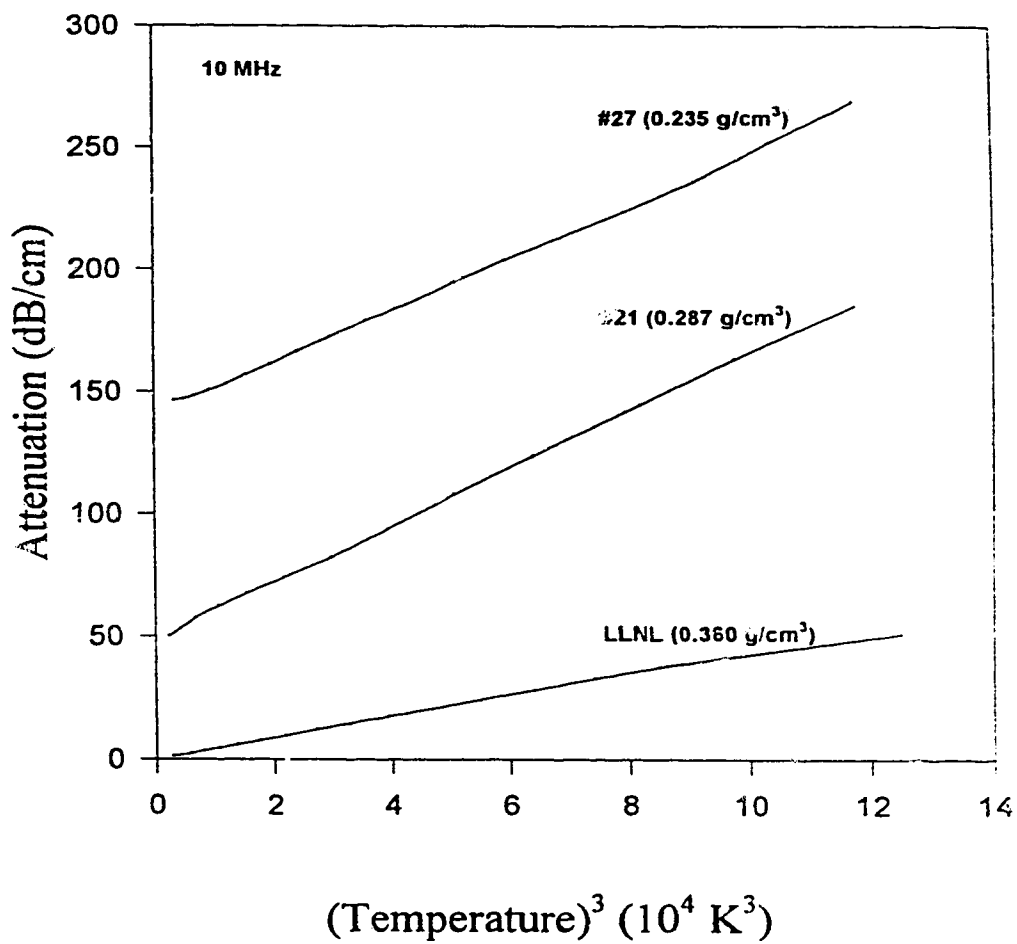Fig. 23 Acoustic absorption of 10 MHz longitudinal wave in aerogels

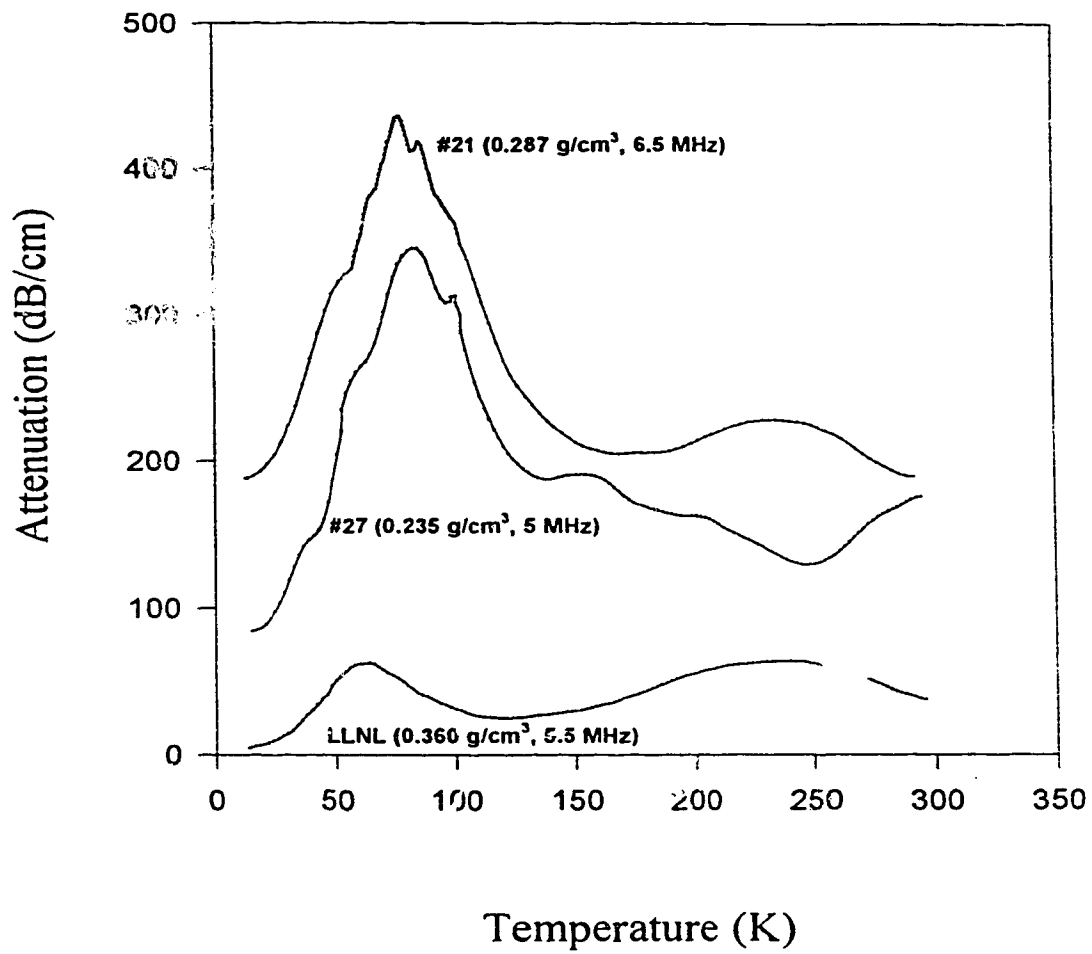Fig. 24 T^3 dependence of acoustic absorption of 10 MHz longitudinal wave in aerogels
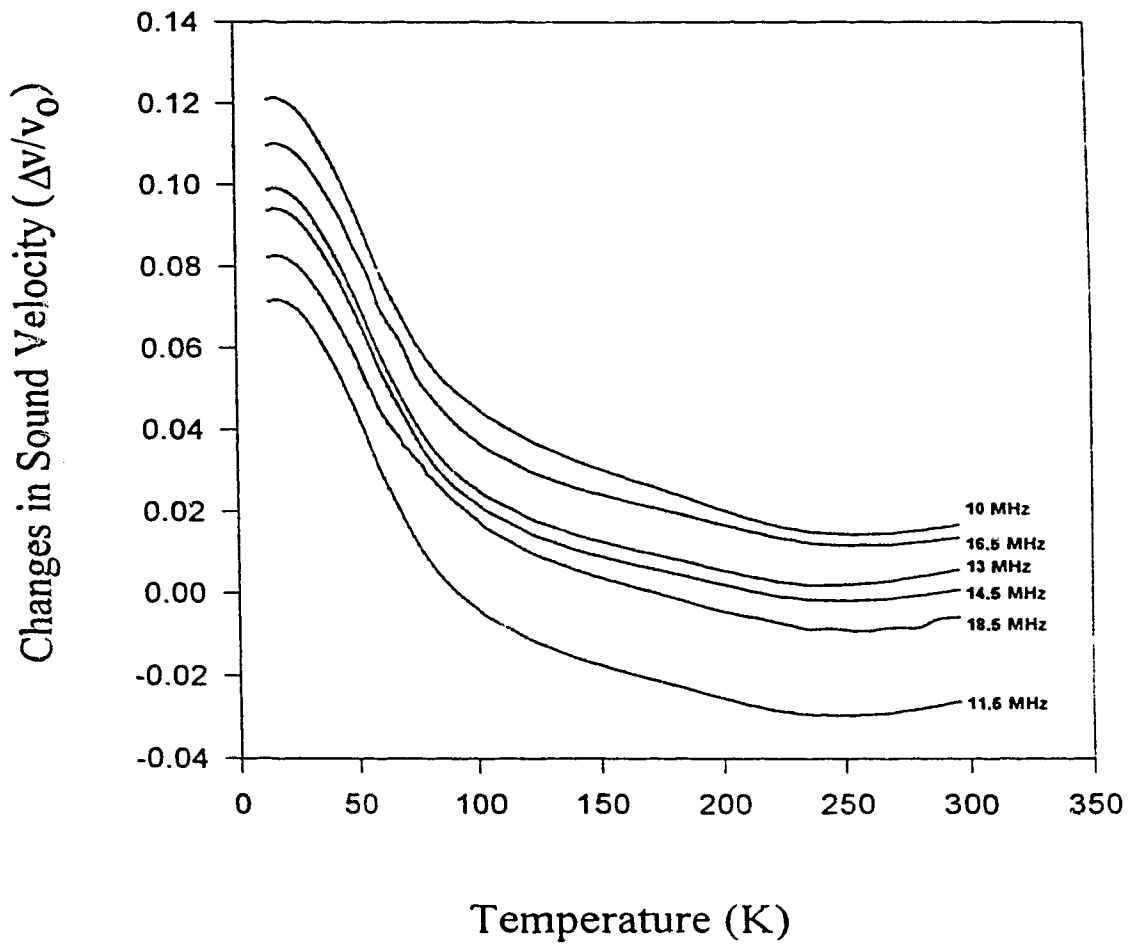
Fig. 25 Acoustic absorption of shear waves in aerogels

Fig. 26 The variations of sound velocities of longitudinal waves in aerogel
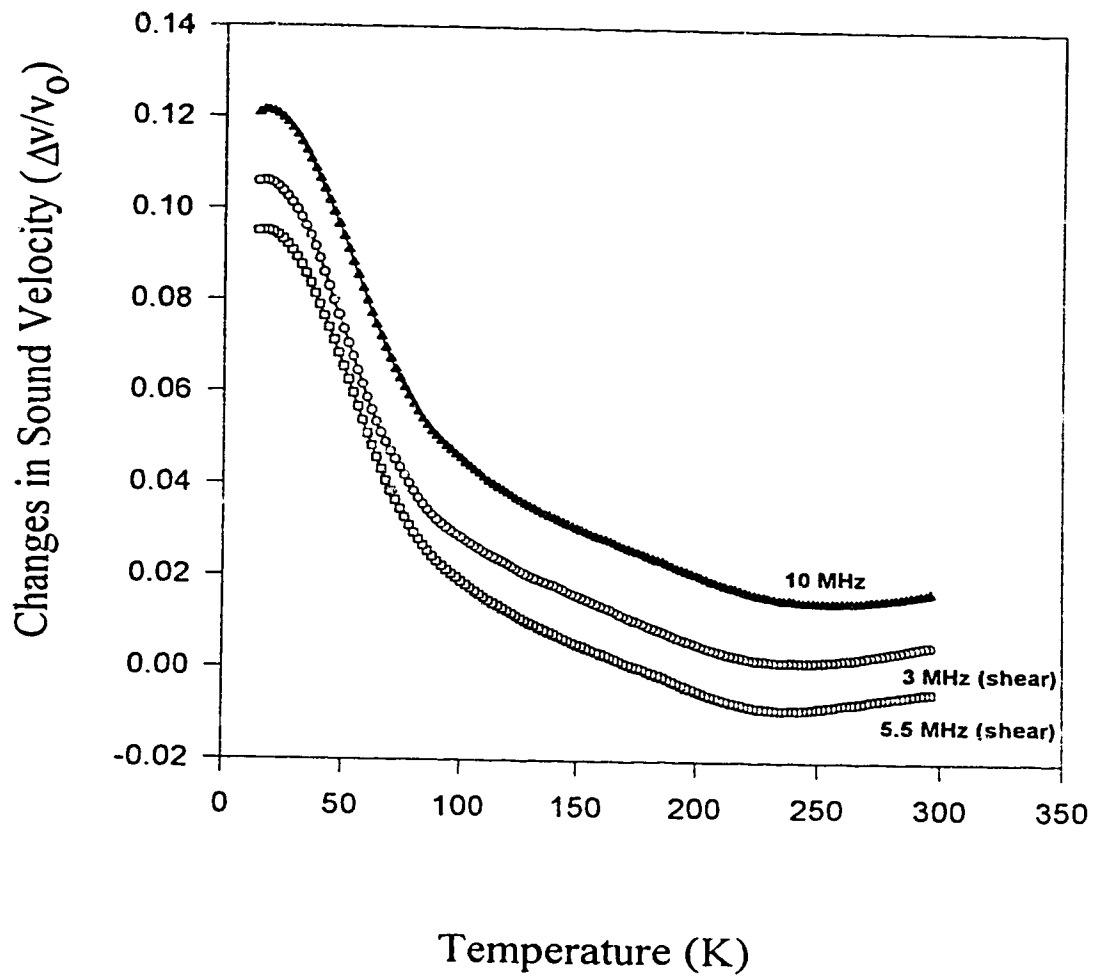
(LLNL, 0.360g/cm³)

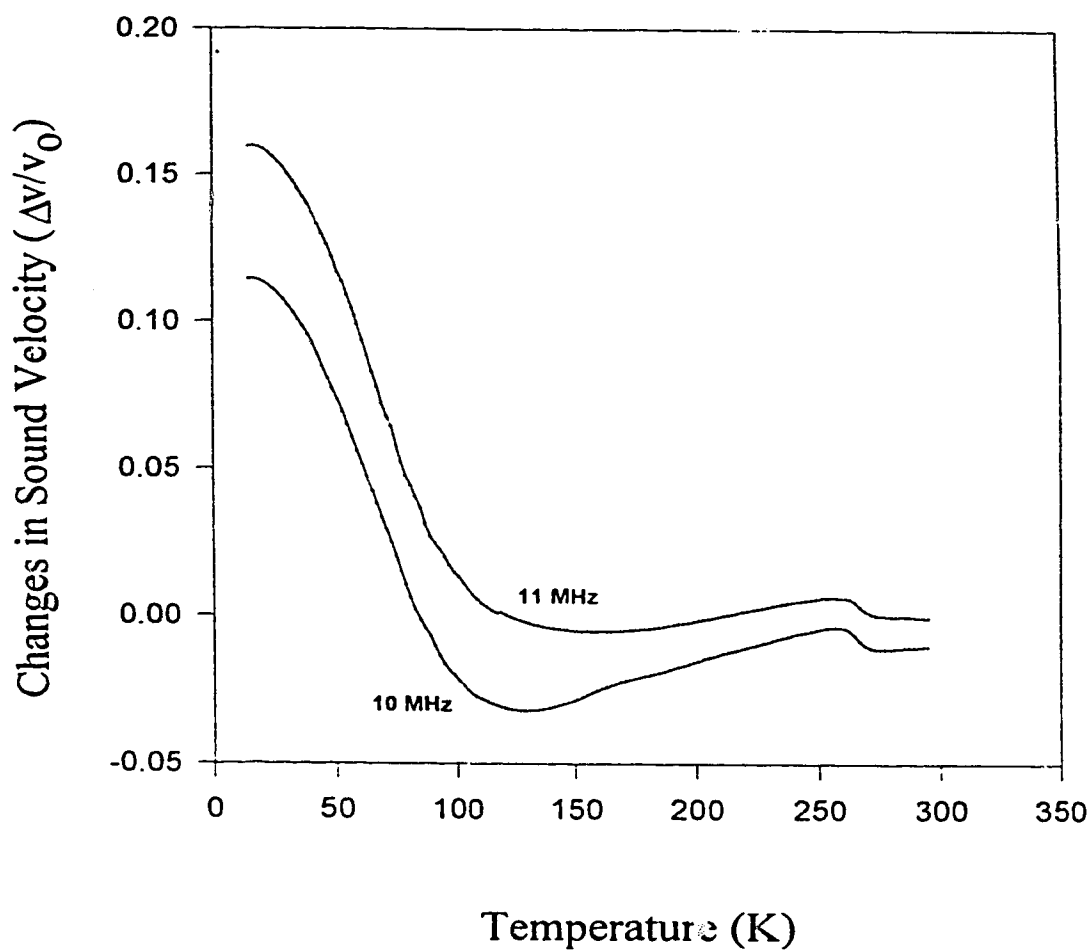Fig. 27 The variations of sound velocity of longitudinal and shear waves in aerogel (LLNL, 0.360 g/cm³)

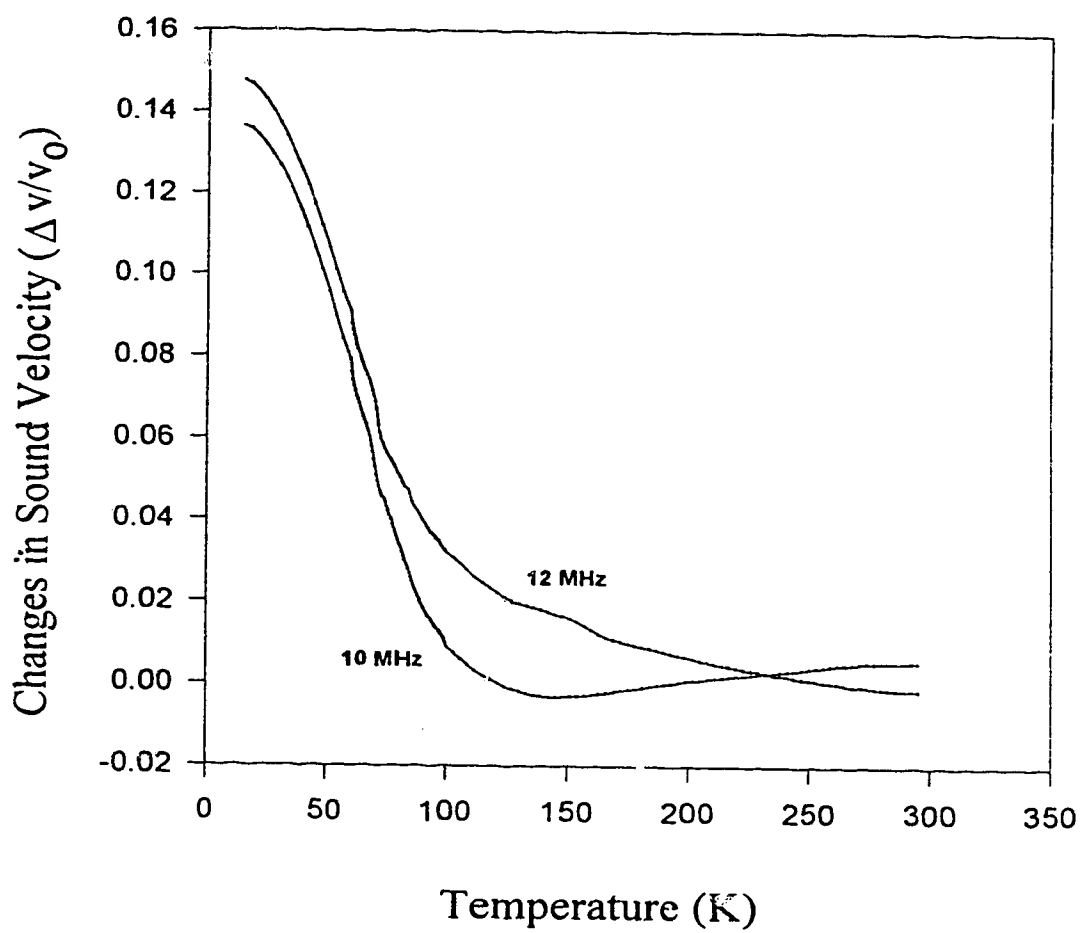Fig. 28 The variations of sound velocity of longitudinal waves in aerogel
(#27, 0.235 g/cm^3)

Fig. 29 The variations of sound velocity of longitudinal waves in aerogel (#21, 0.287g/cm^3)

in different samples are offset for clarity and the "0" here is arbitrary. According to those figures, the changes of sound speed over the whole temperature range are very large, more than 10%, in all samples and for shear as well as longitudinal modes. In the region around the attenuation peaks the velocities increase dramatically with decreasing temperature. There are noticeable differences between the sound velocities in different samples, as shown in Fig. 30. In the samples made here, the changes are much bigger, about 20%, than in the LLNL sample, where they are about 11%. Secondly, there is a minimum in the sound velocity which occurs around 250 K in the LLNL sample and around 100 to 150 K in the other samples. The minimum becomes deeper in lower density samples.

Within the range of these measurements, there is no apparent frequency dependence in the temperature dence of the sound velocity, as can be seen from Fig. 26. From Fig. 27, the changes appear to be about the same for longitudinal and shear modes.

§5.4   Discussion of Ultrasonic Results

As seen above, there is a large attenuation peak around 60 to 80 K in all the aerogel samples. This is qualitatively similar to the behavior of glasses shown in Fig. 5. It appears that aerogels, which are also amorphous, have a similar thermally activated relaxation process. The same conclusion can be drawn from the sound velocities which show a dramatic increase with decreasing temperature in the region where the attenuation peak occurs. This is the
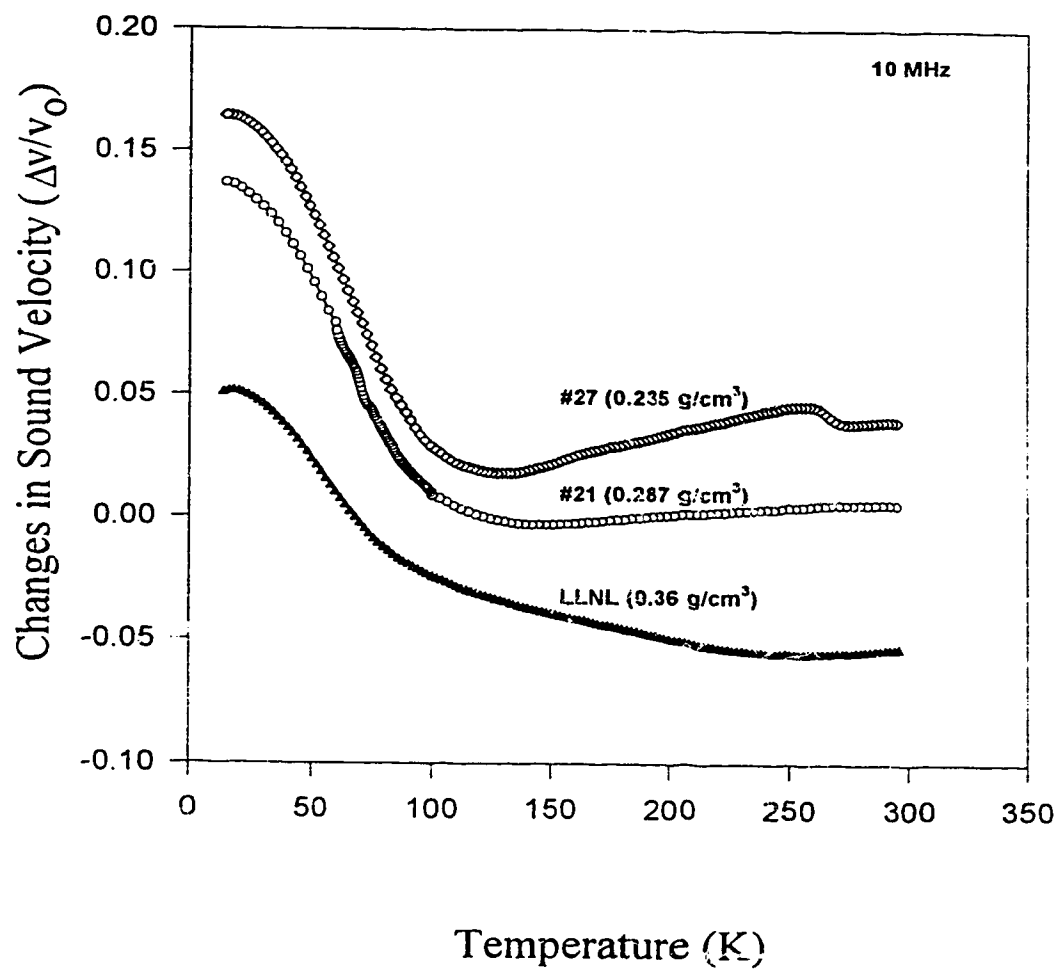
Fig. 30 The variations of sound velocity of 10 MHz longitudinal wave in aerogels

characteristic of a relaxation process as discussed in §3.2. However, it is not clear from the data that there is a frequency dependence of the attenuation peak positions.

Comparing to Fig. 5, the attenuation peak in aerogels is much bigger than in solid glasses. One reason is the very low sound velocity in aerogels. From equation [5], the attenuation (the inverse mean free path) is proportional to $1/v^3$. Since the sound velocity is about an order of magnitude smaller in aerogels than in solid glasses, any relaxation peaks in aerogels would be expected to be much bigger than in glasses. The changes in sound velocity are about 10 times larger than in solid glasses, but the reasons are not clear.

The data from sample #27 also shows a small attenuation peak at high temperature (around 260 K) at all frequencies, Fig. 21. There is a correponding change in the sound velocity, Fig. 28. There may be a second, high temperature relaxation process in sample #27. However, it is only observed in one of the three samples.

Comparing the LLNL sample to the others, the changes in attenuation are about times smaller and the changes in sound speeds about 2 times smaller. There are at least two possible reasons for these differences. One is the density; the LLNL sample has a density of 0.360 g/cm^3, while the others are less than 0.3 g/cm^3. The other difference is the different process used in making the aerogels. The samples made here were not heat-treated after the hypercritical drying process, while most commercial samples are. As mentioned in §3.4, sintered aerogels have higher stiffness and the changes in sound velocity may be smaller.

Chapter 6   CONCLUSIONS

Aerogels have been produced in the porosity range from 87% to 98% by using the one-step method. Of the samples made here, only those with porosity between 87% and 90% have attenuation peaks small enough to permit ultrasonic measurements at all temperatures from room temperature to 14 K. The ultrasonic measurements in this thesis are the first acoustic measurements in aerogels to cover this temperature range. Due to the difficulties of producing samples with high density and in obtaining ultrasonic signals from low density samples, our measurements were restricted to the density range 0.20 to 0.30 g/cm³.

All the samples studied have similar features in the temperature dependence of the attenuation and the sound velocity. There are large attenuation peaks and changes in the sound velocities around liquid nitrogen temperature (60 K - 80 K). The attenuation peaks are much bigger than in non-porous glasses and the changes in sound velocity are also extremely large, as much as 20% in some samples.

Although the general features are similar, the magnitude of the attenuation peaks and the changes in sound velocity are different in different samples. The differences can be seen most clearly by comparing results for samples made here and the LLNL sample. The LLNL sample has much smaller attenuation peaks and velocity changes. Possible reasons include the different densities and the heat treatment of the LLNL sample after hypercritical drying.

Several things can be done to continue this work. Making velocity and attenuation measurements over a wider density range would be useful. The effects of heat treatment and sintering on the acoustic properties should be systematically studied. Better techniques for bonding transducers to aerogels would lessen the damage to the samples, improve the signals and allow measurement over a wider frequency range.

BIBLIOGRAPHY

[1.1]   P.H. Tewari, A.J. Hunt, and K.D. Lofftus, *Aerogels*, ed. J. Fricke, Springer-Verlag, Berlin (1986).

[1.2]   J. Fricke, *Aerogels*, ed. J. Fricke, Springer-Verlag, Berlin (1986).

[1.3]   R. Vacher, T. Woignier, J. Pelous, and E. Courtens, Phys. Rev. B 37, 6500 (1988).

[1.4]   S.B. Kim, J. Ma and M.H.W. Chan, Phys. Rev. Lett. 71, 2268 (1993).

[1.5]   E. Molz, Doctoral dissertation, Univ. Of Alta., (1995).

[1.6]   M.H.W. Chan, K.I. Bium, S.Q. Murphy, G.K.S. Wong. Amd J.D. Reppy, Phys. Rev. Lett. 61, 1950 (1988).

[1.7]   G.K.S. Wong, P.A. Crowell, H.A. Cho, and J.D. Reppy, Phys. Rev. Lett. 65, 2410 (1990).

[1.8]   R. Calemczuk, A.M. De Goer, B. Salce, R. Maynard and Zarembowitch, Eruophys Lett. 3(11), 1205 (1987).

88

[1.9] J. Gross, J. Fricke and L.W. Hrubesh, J. Acoust. Sco., Am.91(4). Pt.1, 2004(1992).

[1.10] A.M de Goer, R. Calemczuk, B.Salce, J. Bon, E. Bonjour and R. Maynard, Phys. Rev., B 40, 8327 (1989).

[2.1] S.S. Kistler, Nature 127, 741(1931).

[2.2] S.J. Teichner, *Aerogels*, ed. J. Fricke, Springer-Verlag, Berlin (1986).

[2.3] G. Poelz and R. Riethmüller, *Neclear Instruments & Methods* 195 491-503 (1982).

[2.4] S. Henning, *Aerogels*, ed. J. Fricke, Springer-Verlag, Berlin (1986).

[2.5] F.A.L. Dullien, *Porous Media*, Academic Press, Harcourt Brace Jovanovich, Publishers, San Diego (1992).

[2.6] S. Brunauer, *The Adsorption of Gas and Vapor*, Princeton Univ. Press, Princeton (1945).

[2.7] G. Schuck, W. Dietrich, and J. Fricke, *Aerogels*, ed. J. Fricke, Springer-Verlag, Berlin (1986).

[2.8] Serway. *Physics for Scientists and Engineers*, Saunders College Publishing, Harcourt Brace College Publishers, Philadephia (1992).

[2.9] O. Nilsson, Å. Fransson, and O. Sandberg, *Aerogels*, ed. J. Fricke, Springer-Verlag, Berlin (1986).

[3.1] Blitz, Butterworths: *Fundametals of Ultrasonics*, Butterworths, London (1963).

[3.2] S.Hunkinger and W. Arnold, *Physical Acoutics*, ed. Warren P. Mason, XII, Academic Press, New York (1976).

[3.3] S. Hunklinger and M.V. Schickfus, *Amorphous Solids*, ed. W.A. Phillips, Springer-Verlag, Berlin (1981).

[3.4] J. Jäckle, L. Piche, W. Arnold & S. Hunklinger, J. Non Cryst. Solids 20, 365-391 (1976).

[3.5] L.F. Nielsen, J. Am. Ceramic Soc., 67, 93 (1983).

[3.6] C.A.M. Muler and J.G. van Lierop, *Aerogels*, ed. J. Fricke, Springer-Verlag, Berlin (1986).

[3.7]   J.R. Beamish, A. Hikata, and C.Elbaum, Phys. Rev., B 27, 5848 (1983).

[4.1]   Jongsoo Yoon: *Fabrication of Aerogel in small scale*, Moses Chan's Group. Dept. Of Phys., Penn State Univ. (unpublished).

[4.2]   Norbert Nuiders: *Helium in Vycor, An Ultrasonic Study*, Doctoral dissertation, Univ. of Delaware (1990).